Computing Approximate Graph Edit Distance via Optimal Transport

QIHAO CHENG[*†], Tsinghua University, China
DA YAN[*], Indiana University Bloomington, USA
TIANHAO WU[*], Tsinghua University, China
ZHONGYI HUANG, Tsinghua University, China
QIN ZHANG, Indiana University Bloomington, USA

Given a graph pair (G^1, G^2), graph edit distance (GED) is defined as the minimum number of edit operations converting G^1 to G^2. GED is a fundamental operation widely used in many applications, but its exact computation is NP-hard, so the approximation of GED has gained a lot of attention. Data-driven learning-based methods have been found to provide superior results compared to classical approximate algorithms, but they directly fit the coupling relationship between a pair of vertices from their vertex features. We argue that while pairwise vertex features can capture the coupling cost (discrepancy) of a pair of vertices, the vertex coupling matrix should be derived from the vertex-pair cost matrix through a more well-established method that is aware of the global context of the graph pair, such as optimal transport. In this paper, we propose an ensemble approach that integrates a supervised learning-based method and an unsupervised method, both based on optimal transport. Our learning method, GEDIOT, is based on inverse optimal transport that leverages a learnable Sinkhorn algorithm to generate the coupling matrix. Our unsupervised method, GEDGW, models GED computation as a linear combination of optimal transport and its variant, Gromov-Wasserstein discrepancy, for node and edge operations, respectively, which can be solved efficiently without needing the ground truth. Our ensemble method, GEDHOT, combines GEDIOT and GEDGW to further boost the performance. Extensive experiments demonstrate that our methods significantly outperform the existing methods in terms of the performance of GED computation, edit path generation, and model generalizability.

CCS Concepts: • **Mathematics of computing → Graph algorithms**; • **Information systems → Information systems applications**.

Additional Key Words and Phrases: Graph edit distance, Optimal transport, Graph neural network

ACM Reference Format:
Qihao Cheng, Da Yan, Tianhao Wu, Zhongyi Huang, and Qin Zhang. 2025. Computing Approximate Graph Edit Distance via Optimal Transport. *Proc. ACM Manag. Data* 3, 1 (SIGMOD), Article 23 (February 2025), 26 pages. https://doi.org/10.1145/3709673

1 Introduction

Graph edit distance (GED) is one of the most widely used graph similarity metrics, which is defined as the minimum number of edit operations that transform one graph to the other. GED has wide

[*]The first three authors contributed equally to this work.
[†]Corresponding author.

Authors' Contact Information: Qihao Cheng, cqh22@mails.tsinghua.edu.cn, Tsinghua University, China; Da Yan, yanda@iu.edu, Indiana University Bloomington, USA; Tianhao Wu, wuth20@mails.tsinghua.edu.cn, Tsinghua University, China; Zhongyi Huang, zhongyih@tsinghua.edu.cn, Tsinghua University, China; Qin Zhang, qzhangcs@iu.edu, Indiana University Bloomington, USA.

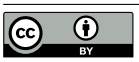

ACM 2836-6573/2025/2-ART23
https://doi.org/10.1145/3709673

applications, such as graph similarity search [25, 52, 61, 66, 69], graph classification [36, 37], and inexact graph matching [7]. Scenarios include handwriting recognition [17], image indexing [54], semantic image matching [51], and investigations of antiviral drugs [67], etc. The lower part of Figure 1 illustrates the edit path (i.e., sequence of edit operations) of a graph pair (G^1, G^2) with GED = 4. The edit path with the minimum length is called Graph Edit Path (GEP), so the length of a GEP is exactly the GED.

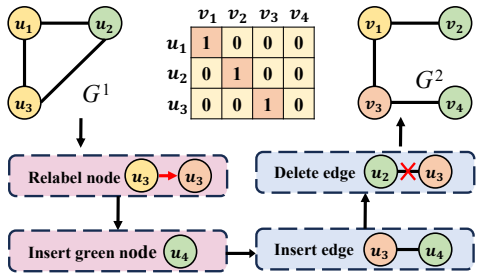

Fig. 1. A toy example of graph pair (G^1, G^2)

Existing methods for GED computation can be categorized into the following three types. **(1) Exact Algorithms.** GED can be computed exactly by the A* algorithm [38], but due to being NP-hard [61], it is time-consuming even for a pair of 6-node graphs [4]. **(2) Approximate Algorithms.** To make computation tractable, approximate algorithms are proposed based on discrete optimization or combinatorial search such as A*-Beam [29], Hungarian [37] and VJ [16]. A*-beam restricts the search space of A* algorithm, which is still an exponential-time algorithm. Hungarian and VJ convert the GED computation to a linear sum assignment problem and find the optimal node matching between two graphs, which takes $O(n^3)$ time. Moreover, these heuristic methods lack a theoretical guarantee and generate results of inferior quality. **(3) Learning-based Methods.** Recent studies turn to data-driven methods based on graph neural networks (GNN) to achieve better performance [2, 3, 33, 35, 59]. Differing from the approximate algorithms, learning-based methods extract intra-graph and inter-graph information by generating node and graph embeddings, which are then used to predict GEDs with smaller errors within $O(n^2)$ time in the worst case. The two most recent works, Noah [59] and GEDGNN [33], further support generating the edit path based on A*-beam search and k-best matching, respectively, to ensure the feasibility of the predicted GED.

However, a key issue remains with these learning-based methods. Specifically, they compute a pairwise vertex discrepancy matrix $\mathbf{A}$ where each element $\mathbf{A}_{i,j}$ corresponds to the coupling cost (discrepancy) of matching vertex i in G^1 to vertex j in G^2, and $\mathbf{A}_{i,j}$ is computed only from their vertex features. As Figure 2(a) shows, a shared operation of all existing learning-based methods (including our GEDIOT) is pairwise scoring, which given two node embedding matrices obtained from G^1 and G^2 (via a graph neural network), returns a matrix $\mathbf{A}$ where element $\mathbf{A}_{i,j}$ is the pairwise score computed from the embeddings of node u_i in G^1 and node v_j in G^2. Here, we use $\oplus$ to denote the pairwise scoring operation. Existing learning-based models directly treat $\mathbf{A}$ as the vertex coupling matrix to fit the ground-truth vertex coupling relationship, but we argue that the coupling matrix should be derived from the pairwise discrepancy matrix $\mathbf{A}$ through a more well-established method that is aware of the global context of the graph pair, such as optimal transport [23]. As illustrated by the bottom branch of Figure 2(b) for GEDGNN [33], they fit $\mathbf{A}$ directly to the 0-1 ground-truth node-matching matrix for GED. Note that the optimal node matching is a global decision: node u_i in G^1 is matched to node v_j in G^2 in the GED solution not only because they have similar labels and neighborhood structures, but also because, for example, node u_i in G^1 is not as

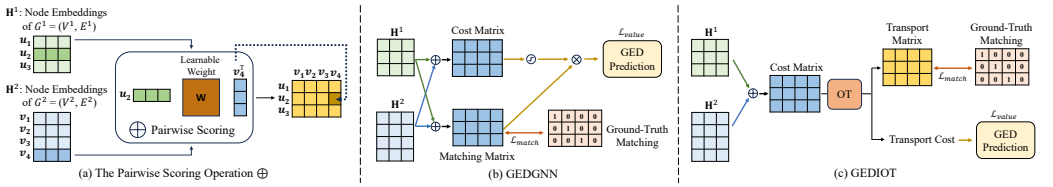

Fig. 2. OT Motivation and Learning-based Model Comparison

similar to the other nodes (e.g., node v_k, $k \neq j$) in G^2. However, $\mathbf{A}_{i,j}$ is computed only based on the embeddings of nodes u_i and v_j.

To fundamentally address this drawback, we propose solutions based on the foundation of the Optimal Transport (OT) theory. OT is a mathematical framework that focuses on finding the most efficient way to move and transform one distribution of mass into another, which has been successfully applied in various fields [13, 23, 57]. Laid upon rigid mathematical theory [31, 47], OT provides strong theoretical guarantees and well-understood properties. With the development of numerical algorithms, such as the Sinkhorn algorithm [14], it is particularly effective and efficient when embedding sentences or graph vertices as probabilistic distributions in the Wasserstein space derived from optimal transport [56, 57].

In this paper, we propose an ensemble approach that integrates a supervised learning-based method and an unsupervised method, both based on OT. Our learning-based method, GEDIOT, is based on inverse optimal transport (IOT) [12, 44] that leverages a learnable Sinkhorn algorithm to generate the coupling matrix. As Figure 2(c) shows, our GEDIOT model takes the cost matrix computed by pairwise scoring, and passes it through an OT module to minimize the cost of transporting masses from nodes of G^1 to nodes of G^2, which returns the learned transport matrix that considers the global cost matrix when fitting the ground-truth node-matching matrix for GED. As our experiments have shown, adding OT after the pairwise-scoring-induced cost matrix brings significant performance improvement in both GED and GEP predictions.

Based on optimal transport, we also propose an unsupervised method, GEDGW, that models GED computation as a linear combination of optimal transport and its variant, Gromov-Wasserstein (GW) discrepancy, for node and edge operations, respectively, which can be solved efficiently without the ground truth. Our ensemble method, GEDHOT, combines GEDIOT and GEDGW to further boost the performance. Our contributions are listed as follows:

- We propose a neural network architecture based on inverse optimal transport (where the cost matrix is learnable) that formulates the GED learning task as a bi-level optimization problem, named GEDIOT (GED with IOT), which introduces the OT component to capture the global context effectively.
- To make OT applicable, GEDIOT extends the learned cost matrix with a dummy row and utilizes the Sinkhorn algorithm with a learnable regularization coefficient to integrate OT with neural networks for GED computation, improving the model performance and stability. Since the coupling matrix can represent the confidence of node matching, we can also generate the edit path from it using the k-best matching algorithm of [33].
- We separate the edit operations into two types: vertex edit operations and edge edit operations. We then model the GED computation as an optimization problem combining optimal transport (for vertex edits) and its variant Gromov-Wasserstein discrepancy (for edge edits), leading to our unsupervised solution named GEDGW (Graph Edit Distance with Gromov-Wasserstein discrepancy).

- We combine GEDIOT and GEDGW into an ensemble method named GEDHOT (Graph Edit Distance with Hybrid Optimal Transport) for more accurate GED computation.
- Extensive experiments show the superior performance of proposed methods. Compared with the state-of-the-art existing method GEDGNN [33], the Mean Absolute Error (MAE) on GED computation decreases by 20.5%–63.8% with GEDIOT. Furthermore, the hybrid method GEDHOT achieves the best performance, where the MAE decreases by 31.2%–72.3% compared with GEDGNN. We also conduct experiments to verify the high-quality edit path generation and superior generalizability of our methods.

The rest of this paper is organized as follows. Section 2 reviews the related work, and Section 3 defines our problem and presents the background of OT. Then, Section 4 describes the proposed learning-based method GEDIOT, and Section 5 further proposes the unsupervised method GEDGW and the ensemble method GEDHOT, and analyzes the time complexity of our methods. Finally, Section 6 reports our experiments, and Section 7 concludes this paper.

2 Related Work

GED Computation. Classical exact algorithms [4, 8] seek the exact graph edit distance for each graph pair. Due to the NP-hardness of GED computation, they fail to generate solutions in a limited time when the graph size increases. To make computation tractable, plenty of heuristic algorithms are proposed, including A*-Beam [29], Hungarian [37] and VJ [16], all of which provide an approximate GED in polynomial time. Recently, graph neural networks (GNN) have become popular since the extracted node and graph embeddings can greatly help the performance in various tasks [24, 50, 55, 62, 63, 65, 70]. A number of GNN-based methods, such as SimGNN [3], TaGSim [2], Noah [59], MATA* [27] and GEDGNN [33], have also been proposed to generate embeddings for GED computation with adequate training data, which achieve the best performance in approximate GED computation. For a more detailed review of heuristic and GNN-based methods, please see Appendix A in our full paper [1].

Graph Similarity Search. Given a query graph and a threshold, graph similarity search retrieves all graphs from a database with GED to the query graph within the given threshold. An important step in this task is to verify whether the GEDs of graph pairs are smaller than the threshold. A series of works [8, 9, 19, 21, 22, 26, 68] are proposed to speed up the GED verification process between the database and the query graph. It is related to, but also distinct from, GED computation. They focus on the filtering technique of search space based on the threshold, while GED computation seeks the difference between a pair of graphs and has no threshold available for filtering. However, when setting the similarity threshold to infinity, the verification step can also be extended for GED computation [8, 9].

Optimal Transport. The goal of optimal transport (OT) [31] is to minimize the cost of transporting mass from one distribution to another. It has been applied in various fields, including image and signal processing [23], natural language processing [57], and domain adaptation [13]. Inverse optimal transport (IOT) [12, 44] is an inverse process to the classical optimal transport, which calculates the cost matrix from the coupling matrix. Recent studies [41, 43] interpret classical contrastive learning as inverse optimal transport. DB-OT [42] applies inverse optimal transport to long-tailed classification. Legal case matching algorithms are proposed in [60] via inverse optimal transport. They all use the general inverse optimal transport with the cross-entropy loss to build an OT-assisted neural network model, and the relation between inverse optimal transport and graphs remains rarely studied as it requires careful design for different graph problems. While our proposed GEDIOT model is also based on IOT, as Section 4.2 will describe, in order for the

Table 1. Notations

Notation	Description
G	a labeled undirected graph
$V,\ E,\ L$	the node, edge and label sets of G
(G^1, G^2)	the graph pair for GED computation
$\mathbf{M}$	node label matching matrix of (G^1, G^2)
$\mathbf{A}^1,\ \mathbf{A}^2$	adjacency matrices of G^1 and G^2
$\mathbf{H}^1,\ \mathbf{H}^2$	final node embeddings of G^1 and G^2
$GED(G^1, G^2)$	the GED of graph pair (G^1, G^2)
$GEP(G^1, G^2)$	the GEP of graph pair (G^1, G^2)
$\boldsymbol{\pi}$	the coupling matrix between G^1 and G^2
$\boldsymbol{\pi}^*,\ GED^*(G^1, G^2)$	ground truths of the graph pair (G^1, G^2)
$\mathbf{1}_n,\ \mathbf{0}_n$	the n-dimensional vectors full of 1 and 0
$\cdot \Vert \cdot$	the concatenation operator
$\cdot \oslash \cdot$	the element-wise division
$\langle \mathbf{P}, \mathbf{Q} \rangle$	the Frobenius dot-product $\sum_i \sum_j (P_{i,j} Q_{i,j})$
$\mathcal{L}(\mathbf{C}^1, \mathbf{C}^2)$	the 4-th order tensor $\left((\mathbf{C}^1_{i,j} - \mathbf{C}^2_{k,l})^2\right)_{i,j,k,l}$
$\mathcal{L} \otimes \mathbf{B}$	the matrix $\left(\sum_{j,l} \mathcal{L}_{i,j,k,l} \mathbf{B}_{j,l}\right)_{i,k}$

Sinkhorn algorithm to be applicable to GED prediction, we need to modify the OT constraints by incorporating a dummy supernode.

A few works have also applied OT and its variants to other graph problems (but not GED) [10, 15, 30, 48, 49]. One of the most important variants is Gromov-Wasserstein discrepancy (GW) [28, 32], a measure used to compare two metric spaces, capturing the differences in their intrinsic geometric structures. GW has been applied for graph partitioning and graph matching [56]. Fused GW [45] is a combination of optimal transport and GW, which has been successfully applied in graph classification and clustering. However, the optimization objective of Fused GW does not consider the edit costs of unmatched vertices in GED computation, but the size of G^1 and G^2 may not match for a given graph pair (G^1, G^2), so as Section 5 will describe, our proposed GEDGW model first needs to add dummy nodes to incorporate such costs into the objective.

3 Preliminaries

This section introduces Graph Edit Distance (GED), Graph Edit Path (GEP), and the fundamental concepts of Optimal Transport (OT) on graphs. All vectors default to column vectors unless otherwise specified. Table 1 summarizes important notations for quick lookup.

3.1 Problem Statement

We consider two tasks: GED computation and GEP generation between two node-labeled undirected graphs $G^1 = (V^1, E^1, L^1)$ and $G^2 = (V^2, E^2, L^2)$. We discuss GED computation of edge-labeled graphs in Appendix H.1 [1] due to space limit. We denote $|V^1| = n_1, |E^1| = m_1$ and $|V^2| = n_2, |E^2| = m_2$. We assume that $n_1 \leq n_2$ as otherwise, we can swap G^1 and G^2.

Graph Edit Distance (GED). Given the graph pair (G^1, G^2), graph edit distance $GED(G^1, G^2)$ is the minimum number of edit operations that transform G^1 to G^2. An edit operation is an insertion/deletion of a node/edge or the relabeling of a node.

Graph Edit Path (GEP). The edit path of the graph pair (G^1, G^2) is a sequence of edit operations that transform G^1 to G^2. The graph edit path $GEP(G^1, G^2)$ is the shortest one with length $GED(G^1, G^2)$.

Figure 1 shows a GEP of the graph pair (G^1, G^2), where different colors denote different vertex labels and $GED(G^1, G^2) = 4$.

Node Matching. The node matching (hereafter we use the terms "node" and "vertex" interchangeably) of (G^1, G^2) is an $n_1 \times n_2$ binary matrix, denoted by $\boldsymbol{\pi} \in \{0,1\}^{n_1 \times n_2}$, where $\boldsymbol{\pi}_{i,k} = 1$ if the node $u_i \in V^1$ matches $v_k \in V^2$, and $\boldsymbol{\pi}_{i,k} = 0$ otherwise. Since we assume that $n_1 \leq n_2$, $\boldsymbol{\pi}$ satisfies the following constraints

$$\boldsymbol{\pi} \mathbf{1}_{n_2} = \mathbf{1}_{n_1}, \quad \boldsymbol{\pi}^\top \mathbf{1}_{n_1} \leq \mathbf{1}_{n_2}, \quad \mathbf{1}_{n_1}^\top \boldsymbol{\pi} \mathbf{1}_{n_2} = n_1, \tag{1}$$

where $\mathbf{1}_n$ is the n-dimensional vector full of 1, and $\mathbf{a} \leq \mathbf{b}$ denotes that $\mathbf{a}_i \leq \mathbf{b}_i$ for the i^{th} elements of $\mathbf{a}$ and $\mathbf{b}$ for all i. Intuitively, the constraints ensure that each of the n_1 vertices of G^1 is matched to a vertex in G^2 since Eq. (1) allows exactly one "1" in each row and at most one "1" in each column. As illustrated in the 0-1 matrix in Figure 1, nodes u_1, u_2 and u_3 in G^1 are matched to v_1, v_2 and v_3 in G^2, respectively, and v_4 in G^2 is not matched.

With a given node matching between G^1 and G^2, the edit path can be generated by traversing and comparing the differences between the labels and edges of all matching nodes in G^1 and G^2. Specifically, (i) we first check each node in G^2 to see if it is matched and if it has the same label as that of its matched node in G^1, if not, we add one to the Edit Distance (ED). This takes $O(n_2)$ time. In Figure 1, since v_3 and u_3 have different labels (hints a node relabeling), and v_4 (hints a node insertion) is not matched, we add 2 to ED. (ii) We then check each edge in G^1 to see if the corresponding edge (decided by the two matched end-nodes) exists in G^2, and vice versa; if not, we add one to ED. This takes $O(m_1 + m_2)$ time. In Figure 1 edge (u_2, u_3) exists in G^1 but the corresponding (v_2, v_3) based on node matching does not exist in G^2 (hints an edge deletion), and edge (v_3, v_4) exists in G^2 but there is no corresponding edge in G^1 (hints an edge insertion), so we add 2 to ED. Overall, the number of edit operations is 4. Note that the time complexity is linear (i.e., $O(n_2 + m_1 + m_2)$). The pseudo-code is shown in Algorithm 3 in Appendix C [1].

By relaxing the binary constraints of $\boldsymbol{\pi} \in \{0,1\}^{n_1 \times n_2}$ to $\boldsymbol{\pi} \in [0,1]^{n_1 \times n_2}$, node matching can be connected with the optimal transport theory to be introduced as follows.

3.2 Background of Optimal Transport

Optimal Transport (OT). The optimal transport problem seeks the most efficient way of transporting one distribution of mass into another. Given a graph pair (G^1, G^2), where $G^1 = (V^1, E^1, L^1)$ and $G^2 = (V^2, E^2, L^2)$, we assume there are two pre-defined mass distributions $\boldsymbol{\mu} = \{\boldsymbol{\mu}_i\}_{i=1}^{n_1}$ and $\boldsymbol{\nu} = \{\boldsymbol{\nu}_j\}_{j=1}^{n_2}$ on nodes of G^1 and G^2, respectively. For instance, when $n_1 = n_2$, for all u_i in G^1 and

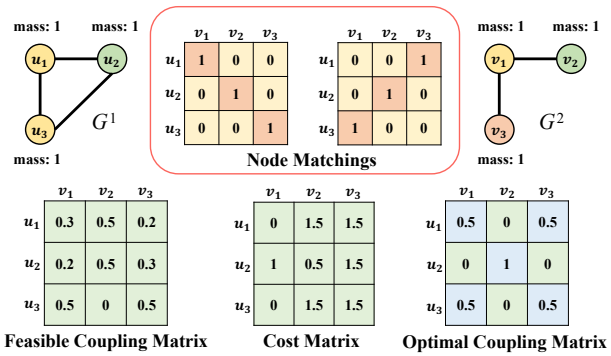

Fig. 3. Example of Cost Matrix and Coupling Matrices

v_j in G^2, we can set their masses as $\boldsymbol{\mu}_i = 1$ and $\boldsymbol{\nu}_j = 1$, which puts the same importance weight on every node. Figure 3 shows our mass distributions on G^1 and G^2 where every node has mass 1. Coupling matrix $\boldsymbol{\pi} \in \mathbb{R}^{n_1 \times n_2}$ is a node-to-node mass transport matrix between G^1 and G^2, where each element $\boldsymbol{\pi}_{i,k}$ denotes the amount of mass transported from node $u_i \in V^1$ to $v_k \in V^2$. In our work, $\boldsymbol{\pi}_{i,k}$ is in the range $[0, 1]$ reflecting the confidence that u_i matches v_k. The feasible set of coupling matrices of (G^1, G^2) is denoted by:

$$\Pi(\boldsymbol{\mu}, \boldsymbol{\nu}) = \left\{ \boldsymbol{\pi} \in \mathbb{R}^{n_1 \times n_2} \mid \boldsymbol{\pi} \mathbf{1}_{n_2} = \boldsymbol{\mu},\ \boldsymbol{\pi}^\top \mathbf{1}_{n_1} = \boldsymbol{\nu},\ \boldsymbol{\pi} \geq 0 \right\}.$$

The lower-left corner of Figure 3 shows an example of a feasible $\boldsymbol{\pi}$. The feasible set of $\boldsymbol{\pi}$ basically relaxes Eq. (1) to allow values in $[0, 1]$, but still requires that elements in a row (resp. column) sum up to 1 (if $n_1 \neq n_2$, dummy nodes need to be added as we will describe in Section 4.2. So we are basically generalizing Eq. (1) for the case when G^1 and G^2 have the same size, where $\boldsymbol{\pi}^\top \mathbf{1}_{n_1} = \mathbf{1}_{n_2}$).

With a given inter-graph node-to-node cost matrix $\mathbf{C} \in \mathbb{R}^{n_1 \times n_2}$, where $\mathbf{C}_{i,j}$ denotes the cost of transporting a unit of mass from $u_i \in V^1$ to $v_j \in V^2$, OT finds the optimal coupling matrix $\boldsymbol{\pi}$ between G^1 and G^2 as follows:

$$\min_{\boldsymbol{\pi} \in \Pi(\boldsymbol{\mu}, \boldsymbol{\nu})} \langle \mathbf{C}, \boldsymbol{\pi} \rangle, \tag{2}$$

where $\langle \mathbf{C}, \boldsymbol{\pi} \rangle = \sum_i \sum_j \mathbf{C}_{i,j} \boldsymbol{\pi}_{i,j}$ is the Frobenius dot-product of $\mathbf{C}$ and $\boldsymbol{\pi}$, and the optimal value is the so-called Wasserstein Distance or Earth Mover's Distance. The lower center of Figure 3 shows a simple hand-crafted cost matrix $\mathbf{C}$ between graphs G^1 and G^2, defined as follows. Initially, we assume matrix $\mathbf{C}$ is all-zero. If the labels of u_i in G^1 and v_j in G^2 are different, we increase $\mathbf{C}_{i,j}$ by 1. Let d_i and d_j be the degrees of u_i and v_j. We further increase $\mathbf{C}_{i,j}$ by $|d_i - d_j|/2$, since the difference between degrees is associated with the number of edge insertions/deletions. The constant $1/2$ is used to avoid double-counting of an edge on its two endpoints. Solving OT over this cost matrix gives the coupling matrix shown in the lower-right corner of Figure 3, which indicates that u_2 is mapped to v_2, but u_1 can be mapped to either v_1 or v_3 with 50% probability each. This directly corresponds to the two optimal node matchings illustrated in Figure 3, which give a GED value of 2. A simple yet efficient method to solve Eq. (2) is by introducing an entropy regularization term into the optimization objective [53]:

$$\min_{\boldsymbol{\pi} \in \Pi(\boldsymbol{\mu}, \boldsymbol{\nu})} \langle \mathbf{C}, \boldsymbol{\pi} \rangle + \varepsilon H(\boldsymbol{\pi}), \tag{3}$$

where $H(\boldsymbol{\pi}) = \sum_i \sum_j \boldsymbol{\pi}_{i,j} \left(\log \boldsymbol{\pi}_{i,j} - 1 \right) = \langle \boldsymbol{\pi}, \log(\boldsymbol{\pi}) - 1 \rangle$ is the entropy function and $\varepsilon > 0$ is the regularization coefficient. Leveraging the duality theory [5] and strict convexity of Eq. (3), the unique solution can be solved by the Sinkhorn algorithm as shown in Algorithm 1 [14], which alternately updates the dual variables $\boldsymbol{\psi}$ and $\boldsymbol{\varphi}$ to fit the specified mass distribution $\boldsymbol{\mu}$ and $\boldsymbol{\nu}$. For more details, please see Appendix B.1 [1].

Gromov-Wasserstein Discrepancy (GW). In practice, it is challenging to define a reasonable node-to-node cost matrix $\mathbf{C} \in \mathbb{R}^{n_1 \times n_2}$ without specified node embeddings for the two graphs G^1 and G^2. To address this issue, Gromov-Wasserstein discrepancy (GW) [28, 64] is introduced for graph alignment tasks [46, 56] as an extension of optimal transport. GW only requires the distances between nodes in the same graph, not inter-graph node distances. Specifically, GW is the optimal value of the following optimization objective:

$$\min_{\boldsymbol{\pi} \in \Pi(\boldsymbol{\mu}, \boldsymbol{\nu})} \sum_{i,j,k,l} (\mathbf{C}^1_{i,j} - \mathbf{C}^2_{k,l})^2 \boldsymbol{\pi}_{i,k} \boldsymbol{\pi}_{j,l}, \tag{4}$$

where $\mathbf{C}^1$ and $\mathbf{C}^2$ are the pre-defined cost matrices (e.g., adjacency matrices, all-pair shortest paths) of graphs G^1 and G^2, respectively. Here, we choose the typical option of $(\mathbf{C}^1_{i,j} - \mathbf{C}^2_{k,l})^2$ to measure the mismatch between two edges $(i, j) \in E^1$ and $(k, l) \in E^2$, but more choices can be found in [32].

Algorithm 1: Sinkhorn algorithm

Input: cost matrix $\mathbf{C}$, mass distributions $\boldsymbol{\mu}$, $\boldsymbol{\nu}$, regularization coefficient ε, maximum iteration *maxiter*

$\mathbf{K} \leftarrow \exp(-\mathbf{C}/\varepsilon)$, $\boldsymbol{\varphi} \leftarrow \mathbf{1}_{n_1}$
for $m = 1$ *to maxiter* **do**
  $\boldsymbol{\psi} \leftarrow \boldsymbol{\nu} \oslash (\mathbf{K}^\top \boldsymbol{\varphi})$
  $\boldsymbol{\varphi} \leftarrow \boldsymbol{\mu} \oslash (\mathbf{K}\, \boldsymbol{\psi})$
$\boldsymbol{\pi} \leftarrow \mathrm{diag}(\boldsymbol{\varphi})\, \mathbf{K}\, \mathrm{diag}(\boldsymbol{\psi})$
$w \leftarrow \langle \mathbf{C}, \boldsymbol{\pi} \rangle$
return $\boldsymbol{\pi}$, w

Intuitively, $\boldsymbol{\pi}_{i,k}$ (resp. $\boldsymbol{\pi}_{j,l}$) represents the probability of matching nodes $u_i \in V^1$ and $v_k \in V^2$ (resp. $u_j \in V^1$ and $v_l \in V^2$), and Eq. (4) computes the expectation of edge-pair mismatch.

Let $\mathcal{L}(\mathbf{C}^1, \mathbf{C}^2)$ be the 4-th order tensor $\left((\mathbf{C}^1_{i,j} - \mathbf{C}^2_{k,l})^2\right)_{i,j,k,l}$ and $\mathcal{L} \otimes \boldsymbol{\pi}$ denotes the matrix $\left(\sum_{j,l} \mathcal{L}_{i,j,k,l} \boldsymbol{\pi}_{j,l}\right)_{i,k}$. Then the objective function can be rewritten into the following simple form:

$$\min_{\boldsymbol{\pi} \in \Pi(\boldsymbol{\mu}, \boldsymbol{\nu})} \left\langle \boldsymbol{\pi}, \mathcal{L}(\mathbf{C}^1, \mathbf{C}^2) \otimes \boldsymbol{\pi} \right\rangle, \tag{5}$$

which can be solved with the conditional gradient algorithm [6, 48].

4 Learning-Based Method: GEDIOT

In this section, we introduce **GEDIOT**, our neural network for GED computation based on inverse optimal transport. The training is an inverse process of OT to find (i.e., fit) the cost matrix given the ground-truth node coupling matrix of (G^1, G^2), $\boldsymbol{\pi}^*$, as supervision.

Motivation of introducing OT. Recall that a node matching satisfies the constraints in Eq. (1). Let us denote its feasible set by

$$U(\mathbf{1}_{n_1}, \mathbf{1}_{n_2}) = \left\{ \boldsymbol{\pi} \geq 0 \mid \boldsymbol{\pi} \mathbf{1}_{n_2} = \mathbf{1}_{n_1},\ \boldsymbol{\pi}^\top \mathbf{1}_{n_1} \leq \mathbf{1}_{n_2},\ \mathbf{1}_{n_1}^\top \boldsymbol{\pi} \mathbf{1}_{n_2} = n_1 \right\}. \tag{6}$$

Previous learning-based models predict GED and node matching via the interaction information of node/graph embeddings [2, 3, 33, 59], but they directly fit the predicted node matching with the ground-truth node coupling using binary cross-entropy loss, without considering all the constraints in $U(\mathbf{1}_{n_1}, \mathbf{1}_{n_2})$ during the training process.

We propose a novel neural architecture, GEDIOT, for GED computation and GEP generation, which predicts only the node-to-node cost matrix $\mathbf{C}$ from the interaction information of node/graph embeddings, and relies on OT to obtain the node matching from $\mathbf{C}$ so that all the constraints in $U(\mathbf{1}_{n_1}, \mathbf{1}_{n_2})$ are taken into consideration.

The training process is constructed as a bi-level optimization as formulated in Eq. (7), where the inner minimization computes the coupling matrix $\widehat{\boldsymbol{\pi}}$ satisfying the constraints in $U(\mathbf{1}_{n_1}, \mathbf{1}_{n_2})$ by solving an entropy-regularized OT problem that can be evaluated with our learnable Sinkhorn module, and the outer minimization calculates the difference between the coupling matrix and the ground truth to update the cost matrix $\widehat{\mathbf{C}}$ via backpropagation.

$$\min_{\widehat{\mathbf{C}}} \ \mathcal{L}_m\left(\boldsymbol{\pi}^*, \widehat{\boldsymbol{\pi}}\right) + \mathcal{L}_v\left(GED^*, \widehat{GED}\right), \tag{7}$$
$$\text{where } \widehat{\boldsymbol{\pi}} = \underset{\boldsymbol{\pi} \in U(\mathbf{1}_{n_1}, \mathbf{1}_{n_2})}{\operatorname{argmin}} \left\langle \widehat{\mathbf{C}}, \boldsymbol{\pi} \right\rangle + \varepsilon H(\boldsymbol{\pi}),$$
$$\widehat{GED} = \left\langle \widehat{\mathbf{C}}, \ \widehat{\boldsymbol{\pi}} \right\rangle.$$

Here, $\boldsymbol{\pi}^*$ and GED^* are the ground truth coupling matrix and GED of graph pair (G^1, G^2), respectively. Note that $\boldsymbol{\pi}^* \in \{0,1\}^{n_1 \times n_2}$ is a one-to-one mapping and there are $(n_2 - n_1)$ full-zero columns. During test, computing GED is simply to solve the (inner) entropy-regularized OT problem, which is thus effective and interpretable.

In Eq. (7), $\widehat{\mathbf{C}} \in \mathbb{R}^{n_1 \times n_2}$ is a learnable cost matrix that encodes the cost of matching each vertex pair across G^1 and G^2, and $\widehat{\boldsymbol{\pi}} \in \mathbb{R}^{n_1 \times n_2}$ denotes the coupling matrix induced from $\widehat{\mathbf{C}}$ by minimizing the inner optimization problem. Recall from Section 3.1 that when relaxing the binary constraints of $\boldsymbol{\pi} \in \{0,1\}^{n_1 \times n_2}$ to $\boldsymbol{\pi} \in [0,1]^{n_1 \times n_2}$, Eq. (1) basically defines $\boldsymbol{\pi}_{i,j}$ to be the probability mass transported from $u_i \in V^1$ to $v_j \in V^2$, and the row $\boldsymbol{\pi}_i$ defines the distribution of transported probability mass from u_i to vertices of V^2. In Eq. (7), the GED value is approximated with $\left\langle \widehat{\mathbf{C}}, \ \widehat{\boldsymbol{\pi}} \right\rangle = \sum_{i=1}^{n_1} \sum_{j=1}^{n_2} \widehat{\mathbf{C}}_{i,j} \widehat{\boldsymbol{\pi}}_{i,j}$ since $\sum_{j=1}^{n_2} \widehat{\mathbf{C}}_{i,j} \widehat{\boldsymbol{\pi}}_{i,j}$ is the expected cost to transport mass from u_i, so $\left\langle \widehat{\mathbf{C}}, \ \widehat{\boldsymbol{\pi}} \right\rangle$ is the expected cost to transport all mass from G^1. In the special case when $\boldsymbol{\pi} \in \{0,1\}^{n_1 \times n_2}$, $\left\langle \widehat{\mathbf{C}}, \ \widehat{\boldsymbol{\pi}} \right\rangle$ basically adds up the costs of transporting mass from u_i to its matched target in V^2 for all $u_i \in V^1$; and the first term in the outer minimization encourages a sparse $\widehat{\boldsymbol{\pi}}$ since the ground-truth $\boldsymbol{\pi}^*$ is sparse.

The objective of the outer optimization contains two terms designed for our two tasks: GED computation and GEP generation. Specifically, $\mathcal{L}_m$ is the matching loss for GEP generation, which we use Binary Cross-Entropy (BCE) loss between the ground truth $\boldsymbol{\pi}^*$ and the learned coupling matrix $\widehat{\boldsymbol{\pi}}$ that is then fed into the k-best matching framework [11, 33] as described in Section 4.5. $\mathcal{L}_v$ is the value loss for GED computation, which we adopt Mean-Squared Error (MSE) between the ground truth GED and the learned one obtained from both node and graph embeddings. The inner entropy-regularized OT of Eq. (7) provides an optimal coupling matrix with the current cost matrix $\widehat{\mathbf{C}}$. Then, the outer minimization fits the learned coupling matrix and GED to the ground truths to optimize the neural parameters in the model. Notably, we will formulate $\widehat{\mathbf{C}}$ further using the node features extracted from (G^1, G^2) by GNN (see Figure 2), so "$\min_{\widehat{\mathbf{C}}}$" in the outer optimization actually optimizes on the parameters of feature extraction network. More analysis of the process of Eq. (7) can be found in Appendix B.2 [1], where we delve into the gap between the learned and ground truth.

Model Overview. Figure 4 illustrates the network architecture of GEDIOT, including three main components: (1) node embedding component, (2) learnable OT component, and (3) graph discrepancy component. We highlight our new OT module with a red dashed frame in Figure 4. In the node embedding component, a GNN is employed to generate node embeddings with multiple graph convolution layers. For both graphs (G^1 and G^2), the node embeddings outputted by all layers are concatenated to aggregate information from neighbors of different hops (instead of only the last-hop neighbors), to alleviate the GNN over-smoothing issue [34, 39]. The concatenated embeddings are then passed through an MLP to derive the final node embeddings of the desired dimension d, denoted by $\mathbf{H}^1 \in \mathbb{R}^{n_1 \times d}$ (for G^1) and $\mathbf{H}^2 \in \mathbb{R}^{n_2 \times d}$ (for G^2). Subsequently, the learnable OT component extracts the node-matching matrix from the node embedding matrices through the OT process. This component includes a cost matrix layer that utilizes $\mathbf{H}^1$ and $\mathbf{H}^2$ to measure the node-to-node

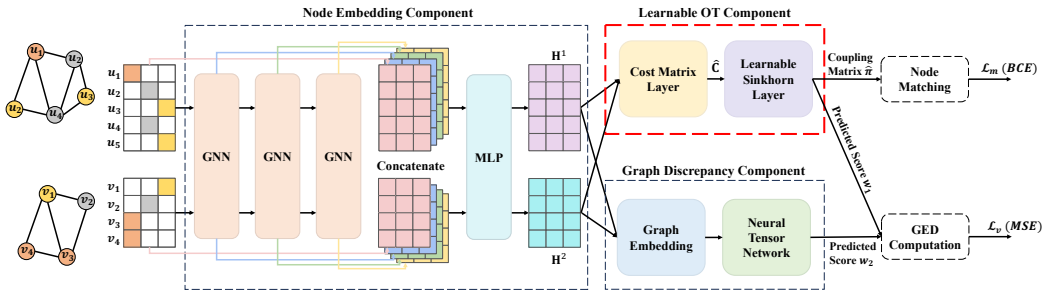

Fig. 4. The architecture of GEDIOT

cost matrix $\widehat{\mathbf{C}}$, and a learnable Sinkhorn layer to read out the learned coupling matrix $\widehat{\boldsymbol{\pi}}$ via the Sinkhorn algorithm with a learnable regularization coefficient. This component also provide a GED score $w_1 = \left\langle \widehat{\mathbf{C}}, \widehat{\boldsymbol{\pi}} \right\rangle$. Additionally, a graph discrepancy component is employed to measure the edit operations of unmatched nodes (e.g., the $(n_2 - n_1)$ nodes in G^2) from the graph-to-graph level, which outputs another score w_2 for GED prediction. This component includes a neural network to generate the graph embeddings and a neural tensor network (NTN) [3] to calculate the predicted score w_2. Finally, scores w_1 and w_2 are combined to compute $GED(G^1, G^2)$. Note that all the sizes of parameters are user-defined (e.g., embedding dimension d) and independent of graph sizes (see more details in Appendix H.2 [1]). Figure 4 marks the learnable parts $(\mathbf{H}^1, \mathbf{H}^2, \widehat{\mathbf{C}}, \widehat{\boldsymbol{\pi}})$ in GEDIOT for ease of understanding.

4.1 Node Embedding Component

In this component, a GNN and an MLP are employed to capture the graph topology information and generate the final node embedding.

GNN Module. We adopt a siamese GNN to generate node embeddings by graph convolution operations, following previous graph similarity learning models [27, 33, 35]. Given the graph pair (G^1, G^2), nodes in both G^1 and G^2 are embedded with the shared network through node feature propagation and aggregation.

Concretely, Graph Isomorphism Network (GIN) [58] is adopted to capture the graph topology, since GIN has been shown to be as powerful as the Weisfeiler-Lehman (WL) graph isomorphism test in differentiating different graph structures [40]. For a graph $G = (V, E, L)$, we initialize the node embedding $\mathbf{h}^{(0)}(u)$ for $u \in V$ as the one-hot encoding of its label. If graphs are unlabeled, we set each initial node embedding as a constant number following previous works [3, 33]. In the i^{th} layer, the embedding of node u, denoted by $\mathbf{h}^{(i)}(u)$, is updated from itself and its neighbors as

$$\mathbf{h}^{(i)}(u) = \text{MLP}\left(\left(1 + \delta^{(i)}\right)\mathbf{h}^{(i-1)}(u) + \sum_{v \in \mathcal{N}(u)} \mathbf{h}^{(i-1)}(v)\right) \tag{8}$$

where $\delta^{(i)}$ is a learnable parameter of each layer and $\mathcal{N}(u)$ is the set of neighbors of u.

MLP Module. As the features propagate via GIN, higher-order graph structural information is fused into node embeddings, which may cause over-smoothed node embeddings at the last layer. Note that various GIN layers contain different orders of topological information: $\mathbf{h}^{(0)}(u)$ represents the features of u itself whereas $\mathbf{h}^{(i)}(u)$ contains the feature information from its i^{th}-hop neighbors. To obtain sufficiently rich node embeddings for more accurate GED computation, we concatenate the node embeddings from all GIN layers: $\mathbf{h} = \left[\mathbf{h}^{(0)} \| \mathbf{h}^{(1)} \| \cdots \| \mathbf{h}^{(k)}\right]$. The concatenated embedding

$\mathbf{h}$ is then fed to an MLP to produce the final node embedding $\mathbf{H} \in \mathbb{R}^{n \times d}$:

$$\mathbf{H} = \text{MLP}(\mathbf{h}) = \text{MLP}\left(\left[\mathbf{h}^{(0)} \| \mathbf{h}^{(1)} \| \cdots \| \mathbf{h}^{(k)}\right]\right). \tag{9}$$

Suppose that the size of input $\mathbf{h}$ is $n \times D$, then we use an MLP with three dense layers of $D \times 2D$, $2D \times D$ and $D \times d$, respectively, to reduce the input $\mathbf{h}$ to the final node embeddings $\mathbf{H} \in \mathbb{R}^{n \times d}$.

4.2 Learnable OT Component

This component includes a cost matrix layer to extract the cost matrix from node embeddings $\mathbf{H}^1$ and $\mathbf{H}^2$ extracted by the node embedding component introduced in Section 4.1, and a learnable Sinkhorn layer to implement the inner entropy-regularized OT of Eq. (7) to generate the node matching from the cost matrix.

Cost Matrix Layer. This layer measures the node-to-node cost matrix $\widehat{\mathbf{C}} \in \mathbb{R}^{n_1 \times n_2}$ for the graph pair (G^1, G^2), by multiplying the final node embeddings $\mathbf{H}^1$, $\mathbf{H}^2$ with a trainable parameter matrix:

$$\widehat{\mathbf{C}} = f\left(\mathbf{H}^1 \mathbf{W} (\mathbf{H}^2)^\top\right),$$

where $\widehat{\mathbf{C}}_{i,j} = f(\mathbf{H}^1_i \mathbf{W} (\mathbf{H}^2_j)^T) = \sum_{k=1}^{d} \sum_{l=1}^{d} f(\mathbf{H}^1_{i,k} \mathbf{W}_{k,l} \mathbf{H}^2_{l,j})$, $\mathbf{W} \in \mathbb{R}^{d \times d}$ is a learnable interaction matrix, and f is an element-wise activation function. $\mathbf{W}_{k,l}$ can be regarded as a correlation weight for the k^{th} dimension in embedding $\mathbf{H}^1$ and the l^{th} dimension in embedding $\mathbf{H}^2$. In this work, we use tanh as the activation function:

$$\widehat{\mathbf{C}} = \tanh\left(\mathbf{H}^1 \mathbf{W} (\mathbf{H}^2)^\top\right). \tag{10}$$

Learnable Sinkhorn Layer. This layer is designed to solve the entropy-regularized OT numerically with the Sinkhorn algorithm in Algorithm 1. It takes the learned cost matrix $\mathbf{C}$ as input to generate the coupling matrix $\widehat{\boldsymbol{\pi}}$ and the predicted score w_1.

Recall that the core process of the Sinkhorn algorithm is the alternate update of dual variables as shown in Lines 3 and 4 in Algorithm 1:

$$\boldsymbol{\psi} \leftarrow \boldsymbol{\nu} \oslash (\mathbf{K}^\top \boldsymbol{\varphi}), \quad \boldsymbol{\varphi} \leftarrow \boldsymbol{\mu} \oslash (\mathbf{K}\, \boldsymbol{\psi}),$$

where $\mathbf{K} = \exp(-\mathbf{C}/\varepsilon)$ is related to the learned cost matrix $\mathbf{C}$ and regularization coefficient ε, $\boldsymbol{\varphi}$ and $\boldsymbol{\psi}$ are the dual variables, and $\boldsymbol{\mu}$ and $\boldsymbol{\nu}$ are the pre-defined mass distributions (e.g., all-1 vectors). However, the constraint set $U(\mathbf{1}_{n_1}, \mathbf{1}_{n_2})$ in Eq. (6) has an inequality constraint $\boldsymbol{\pi}^\top \mathbf{1}_{n_1} \leq \mathbf{1}_{n_2}$, which hinders applying the Sinkhorn algorithm directly, since the derivation of Sinkhorn as detailed in Appendix B.1 [1] only allows equality constraints (with inequality constraints, the dual formulation would introduce additional conditions that require the Lagrangian multipliers to be non-negative for $\boldsymbol{\pi}^\top \mathbf{1}_{n_1} \leq \mathbf{1}_{n_2}$). To address this issue, we reconstruct an equivalent standard-form OT without the inequality constraint by extending the cost matrix $\mathbf{C}$ with a dummy row filled with 0 and redefining mass distributions as $\widetilde{\boldsymbol{\mu}}, \widetilde{\boldsymbol{\nu}}$ as follows:

$$\widetilde{\mathbf{C}} = \begin{bmatrix} \widehat{\mathbf{C}} \\ \mathbf{0}^\top_{n_2} \end{bmatrix}, \quad \widetilde{\boldsymbol{\mu}} = [\mathbf{1}^\top_{n_1},\, n_2 - n_1]^\top, \quad \widetilde{\boldsymbol{\nu}} = \mathbf{1}_{n_2}.$$

Accordingly, we denote the new constraint set by

$$\Pi(\widetilde{\boldsymbol{\mu}}, \widetilde{\boldsymbol{\nu}}) = \left\{\boldsymbol{\pi} \in \mathbb{R}^{(n_1+1) \times n_2} \mid \boldsymbol{\pi} \mathbf{1}_{n_2} = \widetilde{\boldsymbol{\mu}}, \quad \boldsymbol{\pi}^\top \mathbf{1}_{n_1+1} = \widetilde{\boldsymbol{\nu}}, \quad \boldsymbol{\pi} \geq 0\right\},$$

and the standard-form OT is formulated as follows:

$$\min_{\boldsymbol{\pi} \in \Pi(\widetilde{\boldsymbol{\mu}}, \widetilde{\boldsymbol{\nu}})} \left\langle \widetilde{\mathbf{C}}, \boldsymbol{\pi} \right\rangle. \tag{11}$$

Intuitively, the dummy row in $\widetilde{\mathbf{C}}$ basically adds a dummy supernode in G^1 to match $(n_2 - n_1)$ nodes in G^2, as Figure 5 illustrates. We set the cost of matching the dummy supernode as 0 since

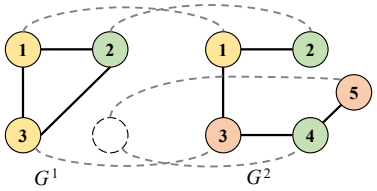

Fig. 5. Illustration of the Dummy Supernode

our learnable OT component only accounts for the edit operations related to node matching (i.e., matching each of the n_1 node in G^1 towards G^2); while the edit cost induced by these $(n_2 - n_1)$ nodes in G^2 will be handled by the graph discrepancy component (see Section 4.3).

By adding entropy regularization $\varepsilon H(\boldsymbol{\pi})$ to Eq. (11), we can solve for $\boldsymbol{\pi}$ by the Sinkhorn algorithm. In each iteration, we update the dual variables $\widetilde{\boldsymbol{\psi}} \in \mathbb{R}^{n_2}$ and $\widetilde{\boldsymbol{\varphi}} \in \mathbb{R}^{n_1+1}$ alternately via:

$$\widetilde{\boldsymbol{\psi}} \leftarrow \widetilde{\boldsymbol{\nu}} \oslash \left(\widetilde{\mathbf{K}}^\top \widetilde{\boldsymbol{\varphi}}\right), \quad \widetilde{\boldsymbol{\varphi}} \leftarrow \widetilde{\boldsymbol{\mu}} \oslash \left(\widetilde{\mathbf{K}} \widetilde{\boldsymbol{\psi}}\right), \tag{12}$$

where $\widetilde{\mathbf{K}} \leftarrow \exp(-\widetilde{\mathbf{C}}/\varepsilon)$ is the element-wise exponential of $-\widetilde{\mathbf{C}}/\varepsilon$. We stack the two operations as feedforward layers to implement the iterations. When the iterative updates converge, $\widetilde{\boldsymbol{\pi}} = \operatorname{diag}(\widetilde{\boldsymbol{\varphi}})\, \widetilde{\mathbf{K}}\, \operatorname{diag}(\widetilde{\boldsymbol{\psi}})$, and the learned coupling matrix $\widehat{\boldsymbol{\pi}}$ is exactly $\widetilde{\boldsymbol{\pi}}$ with the last row removed [10]. The predicted score w_1 is $\left\langle \widehat{\mathbf{C}}, \widehat{\boldsymbol{\pi}} \right\rangle$, which estimates the optimal cost of edit operations induced by node matching.

A question remains: how to set a proper regularization coefficient ε? While a smaller ε leads to a closer approximation of the exact OT solution (without regularization). However, it also introduces a greater risk of numerical instability, which may lead to a divide-by-zero error. A straightforward approach is to set different ε for different datasets manually to achieve satisfactory performance. Nevertheless, the selection of an appropriate ε is costly.

Rather than fixing ε in advance for different datasets, we treat it as a learnable parameter and optimize it by gradient descent during training. The regularization coefficient ε is tuned for different datasets adaptively towards the optimal value, avoiding time-consuming manual adjustments. This is where the term "learnable" in the layer name originated (as Eq. (12) is parameter-free).

We also provide a concrete example from real-world datasets in Appendix D [1] to further illustrate our method.

4.3 Graph Discrepancy Component

Recall that before the learnable Sinkhorn layer, we add a dummy supernode to G^1; when the layer completes and outputs $\widehat{\pi}$, we remove the last row that corresponds to the dummy supernode. The learnable OT component captures only the edit operations induced by the node matching (from the node-to-node level), and some edit operations are not accounted for since $n_1 \leq n_2$. We thus adopt another graph discrepancy component to supplement the unencoded information from the embedding of unmatched $(n_2 - n_1)$ nodes in G^2 from the graph-to-graph level. It includes a graph embedding layer to learn the embeddings of G^1 and G^2, and a neural tensor network (NTN) [3] that reads out the graph discrepancy information from the graph embeddings to enhance GED prediction.

Specifically, we first generate the graph-level embeddings with the node attentive mechanism [3]. Given a graph G (can be either G^1 or G^2) with node embedding matrix $\mathbf{H} \in \mathbb{R}^{n \times d}$ (can be either $\mathbf{H}^1$ or $\mathbf{H}^2$) extracted by our node embedding component, we first calculate the global graph context

vector

$$\mathbf{h}_c = \tanh\left(\mathbf{W}_1\left(\frac{1}{n}\left(\sum_{i=1}^{n}\mathbf{H}_i\right)^\top\right)\right), \tag{13}$$

which averages node features for all nodes of G followed by a non-linear transformation, where $\mathbf{W}_1 \in \mathbb{R}^{d\times d}$ is a learnable weight matrix and $\mathbf{H}_i$ is the i^{th} row of $\mathbf{H} \in \mathbb{R}^{n\times d}$. Then, the attention weight of each node v_i is computed as the inner product between $\mathbf{h}_c$ and $\mathbf{H}_i$ and normalized to the range $(0, 1)$, giving the node weight vector: $\mathbf{a} = \sigma(\mathbf{H}\mathbf{h}_c) \in \mathbb{R}^n$, where σ is the sigmoid function. Finally, the graph embedding $\mathbf{h}_G \in \mathbb{R}^d$ is computed as the weighted sum of node embeddings: $\mathbf{h}_G = \sum_{i=1}^{n}\mathbf{a}_i\mathbf{H}_i$.

Now that we have obtained graph embeddings for G^1 and G^2, we use an NTN to calculate the graph-to-graph interaction vector $\mathbf{s}(G^1, G^2) \in \mathbb{R}^L$ where L denotes the output dimension of NTN.

$$\mathbf{s}(G^1, G^2) = \text{ReLU}\left(\mathbf{h}_{G^1}^\top\mathbf{W}_2^{[1:L]}\mathbf{h}_{G^2} + \mathbf{W}_3[\mathbf{h}_{G^1}^\top \| \mathbf{h}_{G^2}^\top]^\top + \mathbf{b}\right), \tag{14}$$

where $\mathbf{W}_2^{[1:L]} \in \mathbb{R}^{L\times d\times d}$, $\mathbf{W}_3 \in \mathbb{R}^{L\times 2d}$ and $\mathbf{b} \in \mathbb{R}^L$ are learnable, and $\mathbf{h}_{G^1}^\top\mathbf{W}_2^{[1:L]}\mathbf{h}_{G^2}$ denotes the following L-dimensional vector:

$$\left[\mathbf{h}_{G^1}^\top\mathbf{W}_2^{(1)}\mathbf{h}_{G^2}, \quad \mathbf{h}_{G^1}^\top\mathbf{W}_2^{(2)}\mathbf{h}_{G^2}, \quad \ldots, \quad \mathbf{h}_{G^1}^\top\mathbf{W}_2^{(L)}\mathbf{h}_{G^2}\right]^\top,$$

where $\mathbf{W}_2^{(i)}$ is the i^{th} learnable weight matrix of $\mathbf{W}_2^{[1:L]}$.

Finally, we apply an MLP to progressively reduce the dimension of $\mathbf{s}(G^1, G^2)$ to a scalar, which outputs the predicted score w_2 to measure the edit operations of the unmatched nodes.

4.4 Model Training

GEDIOT is supervised by the ground-truth $GED^*(G^1, G^2)$ and the corresponding coupling matrix $\boldsymbol{\pi}^*$ for node matching between two graphs G^1 and G^2 during the training process. As shown in Eq. (7), the loss function consists of two parts: a value loss $\mathcal{L}_v$ to predict the GED and a matching loss $\mathcal{L}_m$ to predict the coupling matrix. The final loss function of GEDIOT is defined as

$$\mathcal{L} = \lambda\mathcal{L}_v + (1-\lambda)\mathcal{L}_m, \tag{15}$$

where we use a hyperparameter λ to balance $\mathcal{L}_v$ and $\mathcal{L}_m$.

Since the range of $GED(G^1, G^2)$ is too large to train a neural network effectively, we normalize the ground-truth GED to the range $[0, 1]$, and the normalized ground-truth GED is given by:

$$\text{n}GED^*(G^1, G^2) = \frac{GED^*(G^1, G^2)}{\max(n_1, n_2) + \max(m_1, m_2)},$$

where the denominator on the right is the maximum number of edit operations that modify all nodes and edges to transform G^1 to G^2. To predict this normalized GED, we define the function:

$$\text{score}(G^1, G^2) = \sigma(w_1 + w_2),$$

where $w_1 = \left\langle \widehat{\mathbf{C}}, \widehat{\boldsymbol{\pi}} \right\rangle$ is the predicted score from the learnable OT component, and w_2 is the predicted score from NTN [3]. Here, σ is the sigmoid function to ensure that the prediction is within $(0, 1)$.

We use MSE as the loss function for value:

$$\mathcal{L}_v = \left(\text{score}(G^1, G^2) - \text{n}GED^*(G^1, G^2)\right)^2,$$

and we fit the predicted coupling matrix with the ground-truth 0-1 matrix $\boldsymbol{\pi}^*$, by minimizing the binary cross-entropy loss (BCE) between the learned coupling matrix $\widehat{\boldsymbol{\pi}}$ and ground truth $\boldsymbol{\pi}^*$:

$$\mathcal{L}_m = \frac{1}{n_1 n_2} BCE\left(\boldsymbol{\pi}^* | \widehat{\boldsymbol{\pi}}\right),$$

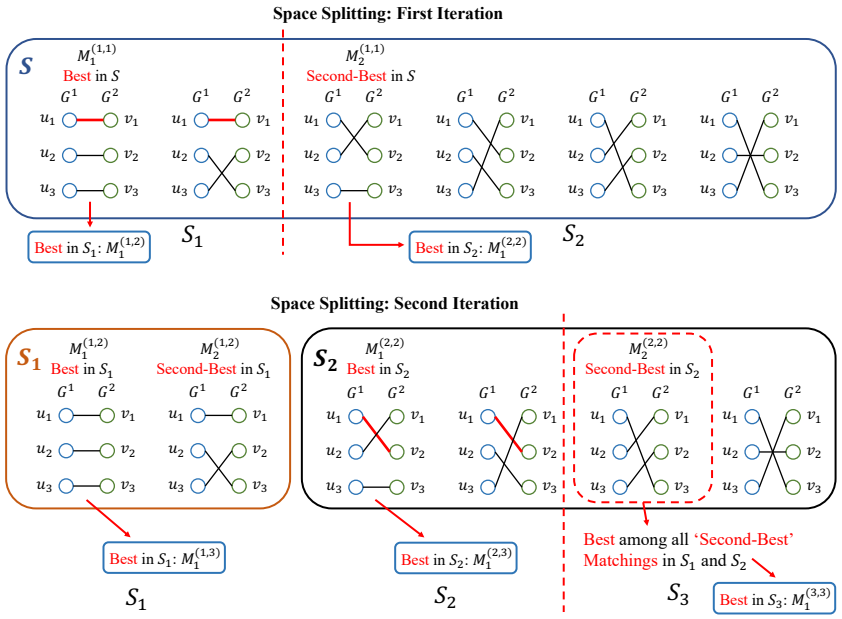

Fig. 6. Example of Space Splitting of k-Best Matching

where

$$BCE\left(\boldsymbol{\pi}^*|\widehat{\boldsymbol{\pi}}\right) = \sum_{i=1}^{n_1}\sum_{j=1}^{n_2} \boldsymbol{\pi}^*_{i,j} \log \widehat{\boldsymbol{\pi}}_{i,j} + \left(1-\boldsymbol{\pi}^*_{i,j}\right) \log\left(1-\widehat{\boldsymbol{\pi}}_{i,j}\right)$$
$$= \left\langle \boldsymbol{\pi}^*,\ \log(\widehat{\boldsymbol{\pi}})\right\rangle + \left\langle 1-\boldsymbol{\pi}^*,\ \log(1-\widehat{\boldsymbol{\pi}})\right\rangle.$$

4.5 GEP Generation

Although we fit $\widehat{\boldsymbol{\pi}}$ to the ground-truth node matching $\boldsymbol{\pi}^* \in \{0,1\}^{n_1\times n_2}$, in practice when the model is trained, the learned coupling matrix $\widehat{\boldsymbol{\pi}}$ outputted by GEDIOT is not perfect but in the range $\boldsymbol{\pi}^* \in [0,1]^{n_1\times n_2}$ representing the confidence of node-to-node matching.

During inference, we adopt the k-best matching framework of [33] to generate $\widehat{GEP}(G^1,G^2)$ from the learned coupling matrix $\widehat{\boldsymbol{\pi}}$, which utilizes the solution space splitting method [11] to obtain a candidate set of k-best bipartite node matchings (based on the matching cost specified by the learned coupling matrix $\widehat{\boldsymbol{\pi}}$) and searches for the one with the shortest edit path as $\widehat{GEP}(G^1,G^2)$. Specifically, let S be a set of node matchings (Figure 6 shows two graphs G^1 and G^2 each having 3 nodes and all 6 possible node matchings in S), in which we can find the best and second-best node matchings according to the matching cost from $\widehat{\boldsymbol{\pi}}$, denoted by $M_1^{(1,1)}$ and $M_2^{(1,1)}$, respectively, in $O(n^3)$ time [11]. The first (resp. second) "1" in the superscript $(1,1)$ means that the two matchings are in the first partition (resp. obtained in the first iteration). Let (u,v) be a node pair in $M_1^{(1,1)}$ but not in $M_2^{(1,1)}$ where $u \in V^1$ and $v \in V^2$. We can split S into two subspaces S_1 and S_2, such that a node matching of S is in S_1 if it contains (u,v), and otherwise it is in S_2. As shown in the upper part of Figure 6, u_1 matches v_1 in the best matching in S, but u_1 does not match v_1 in the second-best matching in S. Then, we split S into S_1 and S_2 according to whether u_1 matches v_1 in the first iteration. Note that $M_1^{(1,1)}$ (resp. $M_2^{(1,1)}$) becomes the best node matching in S_1 (resp. S_2) after splitting, which we denote as $M_1^{(1,2)}$ (resp. $M_1^{(2,2)}$). We also search the new second-best

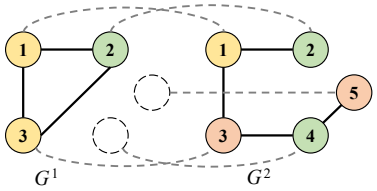

Fig. 7. Illustration of Adding Dummy Nodes in G^1

node matchings in S_1 and S_2, denoted by $M_2^{(1,2)}$ and $M_2^{(2,2)}$, respectively. The entire node matching space is partitioned by repeatedly selecting a partition to split in this manner. Assuming that there are t partitions and each has its best and second-best node matching $M_1^{(r,t)}$ and $M_2^{(r,t)}$, where $r = 1, 2, .., t$, the $(t+1)^{\text{th}}$ best node matching is $M_2^{(t^*,t)}$ of the partition t^* with the best 'second-best' node matching, so partition t^* is selected for splitting. Consider the lower part of Figure 6, where we assume the second-best matching $M_2^{(2,2)}$ in S_2 is better than the second-best matching $M_2^{(1,2)}$ in S_1. Since the best and second-best matchings in S_2 differ based on whether u_1 is matched to v_2, we further split S_2 accordingly. After splitting, the second-best matching $M_2^{(2,2)}$ in the original S_2 becomes the best matching in S_3, which we denote as $M_1^{(3,3)}$. This process is repeated until k partitions are reached, and GED lower-bound-based pruning [8, 18] is integrated to prune the unfruitful branches. Finally, $2k$ node matchings (2 from each partition) are collected as the candidate set to find the shortest edit path. More details can be found in Appendix C [1].

5 Unsupervised Method: GEDGW

Currently, learning-based methods [2, 3, 33, 59] show the best performance of approximate GED computation, but they need ground truth for training set. This section presents our unsupervised optimization approach, **GEDGW**, that is able to achieve performance comparable to learning-based methods. GEDGW is based on the Gromov-Wasserstein discrepancy, which bridges GED computation and optimal transport from an optimization perspective.

5.1 Formulation of GEDGW

Recall that the total edit operations that transform G^1 to G^2 can be determined with a given node matching between G^1 and G^2, where GED is the smallest one. Consequently, the GED computation of the graph pair (G^1, G^2) can be formulated as an optimization problem related to node matching.

Since there can be $(n_2 - n_1)$ nodes in G^2 that do not match any nodes in G^1, we add $(n_2 - n_1)$ dummy nodes in G^1 without any labels and edges following previous works [20, 38], as Figure 7 illustrates. This ensures that the two graphs have the same number of nodes without affecting the GED computation. For simplicity, we abuse the notations to still denote the graph after adding dummy nodes by G^1 and let $n = n_2 = \max\{n_1, n_2\}$ in this section.

Given a node matching, we can derive its induced edit operations into those on nodes and edges. Accordingly, GED computation can be derived by solving the following quadratic programming problem where the first (resp. second) term in the objective models the cost of node (resp. edge) edit operations. Appendix B.3 [1] provides a detailed illustration of the GEDGW formulation.

$$\min_{\boldsymbol{\pi}} \sum_{i,k} \mathbf{M}_{i,k}\boldsymbol{\pi}_{i,k} + \frac{1}{2}\sum_{i,j,k,l}(\mathbf{A}^1_{i,j} - \mathbf{A}^2_{k,l})^2\boldsymbol{\pi}_{i,k}\boldsymbol{\pi}_{j,l}, \tag{16}$$
$$\text{s.t. } \boldsymbol{\pi}\mathbf{1}_n = \mathbf{1}_n, \quad \boldsymbol{\pi}^\top\mathbf{1}_n = \mathbf{1}_n, \quad \boldsymbol{\pi} \in \{0,1\}^{n\times n}.$$

Here, $\mathbf{M} \in \{0,1\}^{n \times n}$ is the node label matching matrix between nodes of G^1 and G^2, where $\mathbf{M}_{i,k} = 1$ if nodes $u_i \in V^1$ and $v_k \in V^2$ have the same label; otherwise $\mathbf{M}_{i,k} = 0$. Matrices $\mathbf{A}^1 \in \{0,1\}^{n \times n}$ and $\mathbf{A}^2 \in \{0,1\}^{n \times n}$ are the adjacency matrices of G^1 and G^2, respectively. The factor $\frac{1}{2}$ in the second term is to avoid the double counting of $\boldsymbol{\pi}_{i,k}\boldsymbol{\pi}_{j,l}$ and $\boldsymbol{\pi}_{j,l}\boldsymbol{\pi}_{i,k}$ since the graphs are undirected.

More concretely, the first linear term of Eq. (16) measures the cost of the node edit operations, including (1) The insertion/deletion of a node as indicated by matching a node in G^2 and a dummy node in G^1, and (2) the relabeling operation as represented by matching a node in G^2 to an original node in G^1 whose labels are different.

The second quadratic term measures the cost of edge insertion/deletion since each element $(\mathbf{A}^1_{i,j} - \mathbf{A}^2_{k,l})^2 \boldsymbol{\pi}_{i,k}\boldsymbol{\pi}_{j,l}$ in the sum measures whether edge $(u_i, u_j) \in E^1$ and edge $(v_k, v_l) \in E^2$ exist simultaneously when u_i matches v_k and u_j matches v_l.

After relaxing the binary constraint to allow elements of $\boldsymbol{\pi}$ to take values in $[0,1]$, the solution $\boldsymbol{\pi}$ represents the confidence of node-to-node matching between G^1 and G^2. Note that Eq. (16) with relaxation on binary variables can be regarded as a linear combination of optimal transport (OT) and Gromov-Wasserstein Discrepancy (GW), where the first linear term models the edit operations on nodes as an OT problem (the right part of Figure 9 in Appendix B.3 [1]) and the second quadratic term models the edit operations on edges as a GW problem (the left part of Figure 9 in Appendix B.3 [1]). So we call this method GEDGW. The optimization problem of GEDGW is reformulated as follows:

$$\min_{\boldsymbol{\pi} \in \Pi(\mathbf{1}_n, \mathbf{1}_n)} \ \langle \boldsymbol{\pi}, \mathbf{M} \rangle + \frac{1}{2} \left\langle \boldsymbol{\pi}, \mathcal{L}(\mathbf{A}^1, \mathbf{A}^2) \otimes \boldsymbol{\pi} \right\rangle \tag{17}$$

where $\Pi(\mathbf{1}_n, \mathbf{1}_n) = \{\boldsymbol{\pi} \in \mathbb{R}^{n \times n} \mid \boldsymbol{\pi}\mathbf{1}_n = \mathbf{1}_n,\ \boldsymbol{\pi}^\top \mathbf{1}_n = \mathbf{1}_n, \boldsymbol{\pi} \geq 0\}$ is the feasible set of coupling matrices. We exploit the Conditional Gradient (CG) method [6, 48] to solve GEDGW, which is presented in detail in Appendix B.4 [1]. An example in Appendix D [1] further illustrates our GEDGW method.

5.2 Further Improvement by Ensembling

Recall that GEDGW and GEDIOT model the GED computation from two different perspectives via optimal transport. To achieve better performance, we combine these two OT-based methods into an ensemble **GEDHOT** (GED with Hybrid Optimal Transport), which combines the results from GEDGW and GEDIOT to enhance the performance of GED computation and GEP generation during test.

Specifically, given an input of graph pair (G^1, G^2), we run GEDGW and GEDIOT to get the GEDs and coupling matrices denoted by $\widehat{GED}_{\text{GW}}(G^1, G^2)$ and $\widehat{\boldsymbol{\pi}}_{\text{GW}}$, $\widehat{GED}_{\text{IOT}}(G^1, G^2)$ and $\widehat{\boldsymbol{\pi}}_{\text{IOT}}$, respectively. Since GED is the minimum number of edit operations, we choose the smaller of $\widehat{GED}_{\text{GW}}(G^1, G^2)$ and $\widehat{GED}_{\text{IOT}}(G^1, G^2)$ as $\widehat{GED}(G^1, G^2)$.

$$\widehat{GED}(G^1, G^2) = \min \left\{ \widehat{GED}_{\text{GW}}(G^1, G^2), \widehat{GED}_{\text{IOT}}(G^1, G^2) \right\}.$$

For GEP generation, we generate the best edit paths via the k-best matching framework [33] from $\widehat{\boldsymbol{\pi}}_{\text{GW}}$ and $\widehat{\boldsymbol{\pi}}_{\text{IOT}}$, respectively, and then choose the shorter one.

5.3 Time Complexity Analysis

Due to space limitation, we provide a comprehensive analysis of the time complexity of our proposed methods in Appendix E [1].

In a nutshell, for GEDIOT, since the model training can be done offline given a graph dataset, we consider the computation cost of its forward propagation, the time complexity of which is given by

$$O\left(N(md + nd^2 + nN^2d^2) + Ld^2 + nd^2 + n^2d + Mn^2\right) \approx O(n^2),$$

Table 2. Statistics of Graph Datasets

$\mathcal{D}$	$\lvert\mathcal{D}\rvert$	$\lvert V\rvert_{avg}$	$\lvert E\rvert_{avg}$	$\lvert V\rvert_{max}$	$\lvert E\rvert_{max}$	$\lvert L\rvert$
AIDS	700	8.9	8.8	10	14	29
LINUX	1000	7.6	6.9	10	13	1
IMDB	1500	13	65.9	89	1467	1

where we assume that the number of GNN layers is N, the dimension of hidden layers of GNN and MLP is d, the output dimension of NTN is L, $n = n_2$, $m = \max(m_1, m_2)$ and M denotes the number of iterations of the Sinkhorn algorithm. As the hyperparameters are regarded as constants, the time complexity can be simplified to $O(n^2)$, which is the same as previous learning-based methods in the worst case. For GEP generation via the k-best matching framework, the time complexity is $O(kn^3)$.

For GEDGW, we use the CG method [6, 48] (see Appendix B.4 [1] for details) to solve Eq. (17). The time complexity of CG is bounded by $O(Kn^3)$, where K is the number of iterations. For GEDHOT, the time complexity is $O(n^2 + Kn^3) = O(Kn^3)$, and the time complexity to generate GEP using the k-best matching framework is $O(kn^3)$. Note that both GEDGW and GEDHOT have the same time complexity as the classical heuristic algorithms (e.g. Hungarian and VJ).

6 Experiment

This section evaluates the performance of our proposed methods and compares with existing approximate GED computing methods. Our code is released at https://github.com/chengqihao/GED-via-Optimal-Transport.

6.1 Datasets

We use three real-world graph datasets: AIDS, Linux, and IMDB. Table 2 summarizes their statistics including the number of graphs ($|\mathcal{D}|$), the average number of nodes ($|V|_{avg}$) and edges ($|E|_{avg}$), the maximum number of nodes ($|V|_{max}$) and edges ($|E|_{max}$), and the number of labels ($|L|$). For graph pairs with no more than 10 nodes, we use the A* algorithm [38] to generate the exact ground truth, and for the remaining graphs with more than 10 nodes, we use the ground-truth generation technique in [2, 33] to generate 100 synthetic graphs for each graph. For each dataset, we sample 60% graphs and pair every two of them to create graph pairs of the training set. As for the test set, we sample 20% graphs; for each selected graph, 100 graphs are randomly chosen from the training graphs to generate 100 graph pairs for the test set. The validation set is formed in the same manner as the test set. Appendix F.1 [1] describes the datasets, data preprocessing, and dataset partitions in detail.

6.2 Compared Methods

Recall that GEDGW is a non-learning approximation algorithm, GEDIOT is a learning-based method, and GEDHOT is a combination of both. We compare them with the classical approximation algorithms and learning-based methods.

Classical Algorithms. We select three representative classical approximate algorithms for GED computation. (1) **Hungarian** [37] is based on the Hungarian method for weighted graph matching which takes cubic time. (2) **VJ** [16] is based on bipartite graph matching which takes cubic time. (3) **Classic** runs both Hungarian and VJ to find the GEPs, and takes the better GEP. We do not include the heuristic A*-beam algorithm [29] since Noah in the paragraph below is an optimized version of A*-beam with better performance.

Learning-based Methods. We choose four state-of-the-art learning-based methods for GED computation. (1) **SimGNN** [3] is the very first learning method applying GNN for GED computation.

(2) **Noah** and **GPN** [59]. Noah employs the well-designed graph path network (GPN) to optimize the search direction of the A*-Beam algorithm [29] to find GEP. Additionally, GPN can also be utilized independently for GED computation only. (3) **TaGSim** [2] categories edit operations to four different types, and learns the number of edit operations in each type to achieve competitive GED approximation. (4) **GEDGNN** [33] is the latest method for both GED computation and GEP generation. See Section 2 for a detailed review.

Our Methods. We propose **GEDIOT**, **GEDGW**, and **GEDHOT** for comparison. The detailed setup can be found in Appendix F.2 [1].

6.3 Evaluation metrics

We consider four kinds of metrics to evaluate the performance, which have been widely used [2, 3, 33, 59].

Metrics for GED Computation. (1) **Mean Absolute Error** (MAE) measures the average absolute error between ground-truth GEDs and approximate GEDs. For a graph pair (G^1, G^2), it is formulated as $|GED^*(G^1, G^2) - \widehat{GED}(G^1, G^2)|$. (2) **Accuracy** measures the ratio of approximate GEDs that equal the ground-truth GEDs after rounding to the nearest integer. (3) **Feasibility** measures the ratio that the approximate GEDs are no less than the ground-truth GEDs, so that a GEP of this length is feasible (i.e., can be found).

Metrics for Ranking. These metrics measure the matching ratio between the ranking results of the approximate GED and the ground truth. They include (4) **Spearman's Rank Correlation Coefficient** (ρ). (5) **Kendall's Rank Correlation Coefficient** (τ). (6) **Precision at** k ($p@k$). The first two metrics focus on global ranks while the last focuses on top k. We use $p@10$ and $p@20$.

Metrics for Path. These metrics measure how well the generated edit path GEP matches the ground-truth GEP^*. They include (7) $Recall = \frac{|GEP \cap GEP^*|}{|GEP^*|}$, (8) $Precision = \frac{|GEP \cap GEP^*|}{|GEP|}$, and (9) F1 score defined as $F1 = 2 \cdot \frac{Recall \cdot Precision}{Recall + Precision}$.

Metrics for Efficiency. (10) Running Time ($sec/100p$), where p = "pairs". It records the time for every 100 graph pairs during test.

6.4 Experimental Results

We evaluate the performance of various methods for both GED computation and GEP generation.

Performance of GED Computation. We first compare our proposed methods (i.e., GEDGW, GEDIOT, and GEDHOT) with the six baselines mentioned in Section 6.2 (Hungarian and VJ are dominated by Classic and are hence omitted due to space limit). We categorize the methods into three types: learning-based methods, non-learning methods, and hybrid methods. We count Noah also as a hybrid method since it combines GPN with A*-Beam.

Table 3 reports the results. We can see that among the learning-based methods, GEDGNN achieves the best performance on all three datasets for value, ranking, and feasibility metrics. Meanwhile, GEDIOT significantly outperforms GEDGNN (as well as the other learning-based baselines) in terms of value and ranking metrics with comparable time consumption. For instance, compared with the state-of-the-art method GEDGNN, the MAE of our proposed GEDIOT is 23.9%, 63.8%, 20.5% smaller on AIDS, Linux, and IMDB, respectively; also, on AIDS, the accuracy of GEDGNN and our GEDIOT is 40.4% and 49.7%, respectively. Note that TaGSim is the most time-efficient (e.g., on AIDS, the training time for an epoch of TaGSim is 151 s, while that of GEDIOT is 581 s) but cannot return high-quality results. We train TaGSim for more epochs so that the total training time of TaGSim is roughly equal to GEDIOT, and the results are similar to that reported in Table 3. On AIDS, Linux, and IMDB, the MAE and accuracy of TaGSim with more training time are 0.816

Table 3. Performance Evaluations of GED Computation.

Datasets	Methods	Value		Ranking				Feasibility ↑	Time ↓
		MAE ↓	Accuracy ↑	ρ ↑	τ ↑	p@10 ↑	p@20 ↑		($sec/100p$)
AIDS	SimGNN	0.880	34.7%	0.841	0.704	0.632	0.741	61.5%	0.279
	GPN	0.924	35.6%	0.816	0.680	0.606	0.713	66.5%	0.245
	TaGSim	0.807	37.4%	0.862	0.730	0.669	0.754	66.2%	**0.087**
	GEDGNN	0.763	40.4%	0.870	0.742	0.716	0.774	72.1%	0.307
	GEDIOT	0.581	49.7%	0.922	0.813	0.814	0.853	73.9%	0.318
	Classic	6.594	3.3%	0.529	0.418	0.545	0.614	**100%**	1.463
	GEDGW	1.247	41.2%	0.789	0.670	0.752	0.765	**100%**	0.430
	Noah	3.164	5.6%	0.704	0.585	0.681	0.721	**100%**	161.023
	GEDHOT	**0.484**	**59.3%**	**0.936**	**0.838**	**0.863**	**0.885**	73.9%	0.745
Linux	SimGNN	0.408	63.3%	0.939	0.856	0.911	0.916	75.6%	0.278
	GPN	0.142	87.1%	0.959	0.896	0.947	0.974	90.5%	0.265
	TaGSim	0.346	69.6%	0.937	0.859	0.888	0.910	85.9%	**0.069**
	GEDGNN	0.094	91.6%	0.961	0.897	0.980	0.976	95.9%	0.282
	GEDIOT	0.034	97.2%	0.969	0.911	0.992	0.995	98.5%	0.326
	Classic	2.471	21.5%	0.785	0.707	0.762	0.835	**100%**	0.915
	GEDGW	1.198	48.1%	0.817	0.705	0.827	0.811	**100%**	0.382
	Noah	1.736	8.4%	0.870	0.798	0.906	0.936	**100%**	71.646
	GEDHOT	**0.026**	**97.9%**	**0.970**	**0.915**	**0.994**	**0.997**	98.5%	0.754
IMDB	SimGNN	1.191	40.4%	0.735	0.648	0.759	0.799	68.1%	0.291
	GPN	1.614	28.2%	0.742	0.668	0.669	0.708	34.3%	0.229
	TaGSim	5.247	14.8%	0.496	0.441	0.666	0.699	47.7%	**0.095**
	GEDGNN	0.735	59.6%	0.859	0.781	0.838	0.856	80.2%	0.305
	GEDIOT	0.584	65.3%	0.930	0.858	0.902	0.912	78.6%	0.347
	Classic	12.980	62.8%	0.764	0.718	0.837	0.831	**100%**	3.483
	GEDGW	0.818	**83.0%**	0.926	0.896	0.968	0.951	93.6%	0.247
	Noah	10.467	38.4%	0.717	0.688	0.755	0.795	**100%**	4816.67
	GEDHOT	**0.506**	69.9%	**0.956**	**0.899**	**0.978**	**0.972**	73.1%	0.607

↑: higher is better, ↓: lower is better **Bold**: best, Underline: runner-up.

and 37.9%, 0.316 and 70.6%, 4.962 and 11.4% respectively, which are still worse than our model. It demonstrates that our experimental setup is sufficient to converge.

For the non-learning methods, Classic and GEDGW, it is obvious that GEDGW achieves much better performance on all the value and ranking metrics with up to 14× faster computational speed. More surprisingly, on AIDS and IMDB, GEDGW even achieves a higher accuracy than the state-of-the-art learning-based method GEDGNN. Note that the training phase for the learning-based methods always takes several hours, while GEDGW does not need that phase and directly outputs results within a second. Moreover, all the learning-based methods need the ground truths of GED and node matching for model training. The performance of GEDGW suggests that it is possible to approximate high-quality GEDs in a non-learning way.

Finally, for the two hybrid methods, Noah and GEDHOT, we can see that compared to Noah, the MAE of our GEDHOT is up to 20× smaller with hundreds of times smaller computational time (recall that Noah runs the expensive A* algorithm). In addition, in Table 3, GEDHOT clearly outperforms all the other methods, followed by the proposed GEDIOT and GEDGW with a consistent second-best performance on all three datasets. For instance, on AIDS, the accuracies of GEDIOT, GEDGW and GEDHOT are 49.7%, 41.2%, and 59.3% respectively, while that of GEDGNN is only 40.4%. This shows that GEDHOT can combine the merits of both GEDIOT and GEDGW to get better results.

Table 4. Performance Evaluations of GEP Generation.

Datasets	Methods	Value		Ranking				Path			Time ↓
		MAE ↓	Accuracy ↑	ρ ↑	τ ↑	p@10 ↑	p@20 ↑	*Recall* ↑	*Precision* ↑	$F1$ ↑	($sec/100p$)
AIDS	Classic	6.594	3.3%	0.529	0.418	0.545	0.614	0.572	0.345	0.423	**1.752**
	Noah	3.164	5.6%	0.704	0.585	0.681	0.721	0.609	0.505	0.548	163.153
	GEDGNN	1.503	42.2%	0.795	0.690	0.849	0.838	0.715	0.646	0.675	56.439
	GEDIOT	1.266	49.9%	0.814	0.715	0.881	0.858	0.756	0.692	0.719	57.857
	GEDGW	0.829	53.2%	0.862	0.774	0.842	0.858	0.715	0.675	0.692	57.102
	GEDHOT	**0.440**	**71.2%**	**0.923**	**0.864**	**0.951**	**0.935**	**0.809**	**0.786**	**0.796**	112.161
Linux	Classic	2.471	21.5%	0.785	0.707	0.762	0.835	0.770	0.541	0.623	**0.954**
	Noah	1.736	8.4%	0.870	0.798	0.906	0.936	0.851	0.772	0.802	73.018
	GEDGNN	0.156	93.5%	0.970	0.954	0.987	0.980	0.917	0.904	0.909	19.317
	GEDIOT	0.114	95.4%	0.976	0.965	0.988	0.987	0.924	0.914	0.918	19.514
	GEDGW	0.591	72.2%	0.898	0.836	0.925	0.887	0.837	0.780	0.802	26.788
	GEDHOT	**0.033**	**98.4%**	**0.994**	**0.990**	**0.992**	**0.996**	**0.928**	**0.924**	**0.926**	47.523
IMDB	Classic	12.980	62.8%	0.764	0.718	0.837	0.831	0.833	0.628	0.654	**3.663**
	Noah	10.467	38.4%	0.717	0.688	0.755	0.795	0.845	0.670	0.682	4864.38
	GEDGNN	3.574	79.6%	0.888	0.859	0.924	0.924	0.907	0.808	0.826	93.893
	GEDIOT	3.638	82.0%	0.903	0.878	0.923	0.928	0.907	0.816	0.831	93.091
	GEDGW	0.374	93.2%	0.969	0.955	0.988	0.983	0.763	0.736	0.744	81.948
	GEDHOT	**0.254**	**95.0%**	**0.983**	**0.972**	**0.995**	**0.993**	**0.946**	**0.927**	**0.933**	170.412

↑: higher is better, ↓: lower is better **Bold**: best, Underline: runner-up.

Performance of GEP Generation. We next compare the performance of GEP generation of the methods above. Note that among the learning-based baselines, Noah and GEDGNN are the only two that can generate GEP, so we include Noah, GEDGNN, and Classic as baselines in Table 4 for comparison. We can see that Classic takes the shortest computational time, but the MAE is several times larger than other methods. Among the other four methods, similar to GED results in Table 3, GEDHOT achieves the best performance for value and ranking metrics on all the three datasets. For example, on AIDS, the accuracy of GEDGNN and GEDHOT is 42.2% and 71.2% respectively; also, on Linux, GEDHOT obtains 4.7×, 17.9×, 3.5× smaller MAE compared with GEDGNN, GEDGW, GEDIOT, respectively. Moreover, the second-best is either GEDIOT or GEDGW.

Note that the computational time of GEDHOT is about twice as large as the time of the other three methods except for Classic. Even if a smaller time cost is preferred, our proposed GEDGW and GEDIOT are preferred compared to GEDGNN, which is the latest method for GEP generation. It is worth noting that on AIDS and IMDB, the non-learning method GEDGW even achieves 1.8× and 9.6× smaller MAE than the learning-based method GEDGNN.

Regarding path quality metrics, Recall, Precision, and F1 score, Table 4 shows that GEDHOT consistently performs the best, and GEDIOT is consistently the second-best.

We also study the contribution of GEDIOT and GEDGW for the ensemble method GEDHOT. For example, on AIDS, for GED computation, most graph pairs (80.8%) use the results from GEDIOT instead of GEDGW. For GEP generation, 63.1% of the graph pairs use the results from GEDIOT, and 36.9% of the graph pairs use the results from GEDGW. More results can be found in Appendix G.2 [1].

Note that GED is a distance metric, satisfying the triangle inequality. Without loss of generality, we conduct experiments on AIDS and Linux to evaluate the fraction of triangle inequality violations in the predicted GEDs. The results shown in Appendix G.2 [1] indicate that our methods satisfy this property in most cases (> 95%).

6.5 Generalizability

Since all the learning-based methods require training data supervision, it is interesting to explore how they generalize beyond the training data distribution, including our GEDIOT model.

Table 5. GED Computation of Unseen Graph Pairs.

Datasets	Methods	Value		Ranking				Feasibility ↑	Time ↓
		MAE ↓	Accuracy ↑	ρ ↑	τ ↑	p@10 ↑	p@20 ↑		($sec/100p$)
AIDS	SimGNN	0.925	34.4%	0.808	0.668	0.631	0.731	63.6%	0.284
	GPN	1.038	33.4%	0.771	0.631	0.578	0.683	64.5%	0.235
	TaGSim	0.880	34.8%	0.832	0.694	0.674	0.739	66.0%	**0.093**
	GEDGNN	0.826	38.0%	0.831	0.696	0.702	0.750	69.4%	0.298
	GEDIOT	**0.684**	**44.5%**	**0.897**	**0.776**	**0.791**	**0.835**	**71.3%**	0.313
Linux	SimGNN	0.399	63.2%	0.953	0.877	0.934	0.918	77.6%	0.288
	GPN	0.147	86.6%	0.973	0.916	0.948	0.967	90.5%	0.279
	TaGSim	0.347	69.3%	0.951	0.877	0.878	0.905	87.4%	**0.079**
	GEDGNN	0.122	89.8%	0.965	0.904	0.968	0.973	95.1%	0.291
	GEDIOT	**0.051**	**96.1%**	**0.976**	**0.925**	**0.983**	**0.990**	**97.6%**	0.336
IMDB	SimGNN	1.236	39.3%	0.733	0.642	0.755	0.801	67.4%	0.307
	GPN	1.635	27.7%	0.741	0.664	0.670	0.710	33.9%	0.226
	TaGSim	4.811	15.4%	0.501	0.445	0.665	0.700	47.2%	**0.107**
	GEDGNN	0.743	59.2%	0.858	0.777	0.842	0.857	**79.8%**	0.294
	GEDIOT	**0.595**	**65.5%**	**0.925**	**0.850**	**0.903**	**0.913**	78.5%	0.353

↑: higher is better, ↓: lower is better **Bold**: best, Underline: runner-up.

Modeling GED Computation of Unseen Graphs. Recall that we prepared the test set by sampling 100 training graphs for each test graph, which models the graph similarity search task. To evaluate the generalizability, now we instead sample 100 test graphs (rather than training graphs) for each test graph, so that both graphs in a graph pair of the test set are unseen during training.

Table 5 shows the results of the five learning-based methods, where GEDIOT still significantly outperforms GEDGNN and the others in terms of value and ranking metrics. For example, on Linux, the MAE of GEDIOT is 2.4× smaller than GEDGNN, and the accuracy reaches 96.1% while that of GEDGNN is below 90%.

Compared with the results in Table 3, the performance of all methods decreases since the test set is more challenging. Nevertheless, the amount of degradation is not significant. For example, the accuracy of GEDIOT decreases by 10.5% and 1.1% on AIDS and Linux, respectively, which demonstrates its generalizability.

Generalization to Large Unseen Graphs. Ground truth is crucial for supervised learning-based methods. In GED computation, ground truth is difficult to obtain for large graphs due to the NP-hardness of the problem. For instance, there are plenty of graphs with more than 10 nodes in the IMDB dataset, and it is too expensive to calculate the GEDs of these graph pairs with exact algorithms. Therefore, we consider training the model only with small graphs and testing the performance of the learning-based methods on large unseen graphs. More concretely, we select the graph pairs from the training set of IMDB that are formed by the small graphs (at most 10 nodes) to build a new training set. All the methods trained on it are appended with the "-small" suffix, i.e., **GEDGNN-small**, **GEDIOT-small** and **GEDHOT-small**. To evaluate generalizability, we also construct a new test set, which consists of the graph pairs from the test set of IMDB that are formed by the large graphs (more than 10 nodes). The results are shown in Figure 8, where GEDGNN, GEDIOT, and GEDHOT denote the methods trained on the complete training set of IMDB. We can see that models trained on small graphs have an inferior performance compared to training on complete training set. However, GEDHOT-small and GEDIOT-small are still significantly better than GEDGNN-small in terms of MAE and accuracy. Notably, GEDGW achieves the highest accuracy of

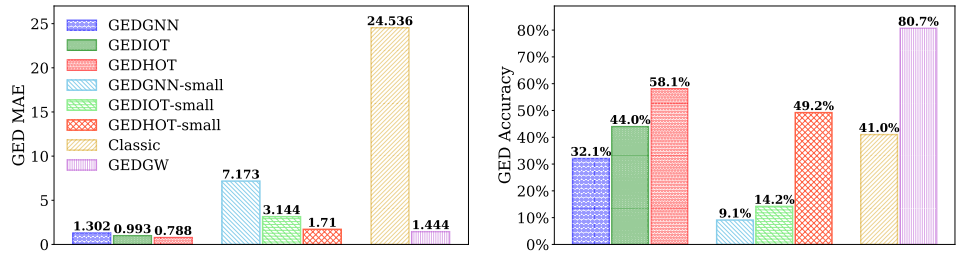

(a) IMDB - MAE (b) IMDB - Accuracy

Fig. 8. Generalizability for Large Unseen Graphs on IMDB

Table 6. Ablation Study of GEDIOT Components.

Method	AIDS						Linux					
	MAE ↓	Accuracy ↑	ρ ↑	τ ↑	p@10 ↑	p@20 ↑	MAE↓	Accuracy ↑	ρ ↑	τ ↑	p@10 ↑	p@20 ↑
GEDIOT	0.581	49.7%	0.922	0.813	0.814	0.853	0.034	97.2%	0.969	0.911	0.992	0.995
GEDIOT (w/ GCN)	0.578	49.1%	0.917	0.805	0.794	0.838	0.064	93.8%	0.967	0.909	0.980	0.985
GEDIOT (w/o MLP)	0.854	35.9%	0.814	0.677	0.599	0.678	0.158	85.9%	0.958	0.889	0.934	0.956
GEDIOT (w/o Cost)	0.794	38.4%	0.870	0.741	0.692	0.765	0.132	87.5%	0.964	0.901	0.953	0.966
GEDIOT (w/o learnable ε)	0.767	38.5%	0.906	0.790	0.801	0.831	0.063	94.7%	0.967	0.910	0.988	0.991

80.7% since it is unsupervised, demonstrating its robustness as compared to learning-based methods that face generalizability challenges.

We further discuss how the generalizability is impacted when synthesizing test graph pairs with larger GEDs. Similarly, GEDGW achieves the best performance and our neural model outperforms GEDGNN. Detailed results are shown in Figure 12 in Appendix G.1 [1].

We notice that the state-of-the-art methods Nass [21] and AStar-BMao [9] for graph similarity search (introduced in Section 2) can be applied for exact GED computation by setting the similarity threshold to infinity. As indicated in [33], exact methods suffer from huge computation costs when the graph size increases. We compare our method GEDIOT with Nass and AStar-BMao on two large real-world datasets. The detailed setup and the running time of the three methods can be found in Appendix G.3 [1]. We find that the running time of the two exact methods Nass and AStar-BMao is quite sensitive w.r.t. the graph size and the GED value. Our method GEDIOT shows a consistent advantage compared to the two exact algorithms, particularly for larger graphs and GEDs, since the time complexity of GEDIOT is only $O(n^2)$, whereas AStar-BMao and Nass are still exponential-time algorithms.

We also generate synthetic power-law graphs of various sizes (from 50 to 400 nodes). The results are reported in Appendix G.4 [1], where we find that the GED relative error of our GEDGW and GEDHOT is nearly 0 while that of GEDGNN is always almost 2, and the computational time of learning-based methods is orders of magnitude faster than the exact algorithms.

6.6 Ablation and Parameter Study

We conduct ablation study to verify the effectiveness of various modules in GEDIOT, and to show the robustness of GEDIOT w.r.t. hyperparameters by varying their values.

Effect of Modules in GEDIOT. In this ablation study, we modify GEDIOT into four variants and compare their performance with GEDIOT. Table 6 shows the results, where we use "w/ GCN" to denote the variant substituting GIN with GCN in GEDIOT, and use "w/o MLP", "w/o Cost", and "w/o learnable ε" to denote GEDIOT that removes the MLP in the node embedding component, that replaces cost matrix module in the learnable OT component with $\mathbf{H}^1(\mathbf{H}^2)^\top$ (i.e., to model

node interactions with simple inner product of their embeddings), and that fixes the regularization coefficient ε in the learnable Sinkhorn layer as $\varepsilon_0 = 0.05$, respectively.

As Table 6 shows, replacing or removing a module in GEDIOT can significantly degrade the performance of both value and ranking metrics, which verifies the effectiveness of our proposed components for GED computation. For instance, on AIDS, if fixing the regularization coefficient ε, the accuracy decreases from 49.7% to 38.5% and MAE increases from 0.581 to 0.767.

Varying Parameters in the Sinkhorn Algorithm. We study how the performance of GEDIOT is impacted as the initial value of the regularization coefficient, denoted by ε_0 and the number of iterations varies in the learnable Sinkhorn layer. The results are presented in Appendix G.5 [1]. We find that both MAE and accuracy are stable with various ε_0, which shows the robustness of the learnable regularization method to ε_0. Moreover, we observe that the MAE decreases and the accuracy increases as the number of iterations increases, but after 15 (resp. 10) iterations on AIDS (resp. Linux), the MAE and accuracy become fairly stable as the Sinkhorn algorithm converges. Note that the computational time also increases when conducting more iterations. Considering the time-accuracy tradeoff, we set the iteration number to 5 by default.

Varying λ in the Loss Function. As presented in Appendix G.5 [1], we also discuss the effect of varying λ in Eq. (15) (from 0 to 1) that balances the two terms $\mathcal{L}_m$ and $\mathcal{L}_v$ of the loss function. The results show that the performance improves with the increase of λ in $[0, 1]$ and becomes stable when λ is around 0.8.

Varying the Size of Training Set. In this experiment, we evaluate the effect of varying the training set size. Concretely, we randomly sample 10%-100% of the original training set of AIDS and Linux to retrain GEDIOT. The results in Appendix G.5 [1] describe its influence on training time, MAE, and accuracy of GEDIOT. It can be observed that as the training set size increases, the MAE decreases and the accuracy increases, while the training time increases linearly. Furthermore, the observed trends of MAE and accuracy with increasing training set size appear to be flattening, which shows that training set size is sufficient.

k-Best Matching. We further verify the effect of k in k-best matching for GEP generation. As depicted in Appendix G.5 [1], the MAE constantly decreases and the accuracy increases as the parameter k increases. Nevertheless, computational time also increases with the increase of k since the search space becomes larger.

7 Conclusion

In this paper, we proposed novel optimal-transport-based methods for graph edit distance computation and graph edit path generation from both learning and optimization perspectives. We first proposed a neural network with inverse optimal transport called GEDIOT. By modeling the node edit operations and edge edit operations as optimization problems, we also proposed an unsupervised method GEDGW to approximate the GED value without the need of training. Additionally, we combine the two methods and propose an ensemble method GEDHOT which achieves a higher performance. Experiments demonstrate that our methods outperform the state-of-the-art methods for GED computation and GEP generation with remarkable result quality and generalizability.

Acknowledgments

This work was supported by DOE ECRP Award 0000274975, NSF OIA-2229394, NSF OAC-2414474, and NSF OAC-2414185. Additionally, Zhongyi Huang was partially supported by the NSFC Project No. 12025104.

References

[1] 2024. Full Technical Report. https://arxiv.org/abs/2412.18857.

[2] Jiyang Bai and Peixiang Zhao. 2021. TaGSim: Type-Aware Graph Similarity Learning and Computation. *PVLDB* 15, 2 (2021), 335–347.

[3] Yunsheng Bai, Hao Ding, Song Bian, Ting Chen, Yizhou Sun, and Wei Wang. 2019. SimGNN: A Neural Network Approach to Fast Graph Similarity Computation. In *WSDM*. 384–392.

[4] David B Blumenthal and Johann Gamper. 2020. On The Exact Computation of The Graph Edit Distance. *Pattern Recognition Letters* 134 (2020), 46–57.

[5] Stephen Boyd and Lieven Vandenberghe. 2004. *Convex Optimization*. Cambridge University Press.

[6] Gábor Braun, Alejandro Carderera, Cyrille W Combettes, Hamed Hassani, Amin Karbasi, Aryan Mokhtari, and Sebastian Pokutta. 2022. Conditional Gradient Methods. *arXiv preprint arXiv:2211.14103* (2022).

[7] Horst Bunke and Gudrun Allermann. 1983. Inexact Graph Matching for Structural Pattern Recognition. *Pattern Recognition Letters* 1, 4 (1983), 245–253.

[8] Lijun Chang, Xing Feng, Xuemin Lin, Lu Qin, Wenjie Zhang, and Dian Ouyang. 2020. Speeding up GED Verification for Graph Similarity Search. In *ICDE*. 793–804.

[9] Lijun Chang, Xing Feng, Kai Yao, Lu Qin, and Wenjie Zhang. 2022. Accelerating Graph Similarity Search via Efficient GED Computation. *IEEE Transactions on Knowledge and Data Engineering* 35, 5 (2022), 4485–4498.

[10] Laetitia Chapel, Mokhtar Z Alaya, and Gilles Gasso. 2020. Partial Optimal Transport with Applications on Positive-unlabeled Learning. *NeurIPS* 33 (2020), 2903–2913.

[11] Chandra R Chegireddy and Horst W Hamacher. 1987. Algorithms for Finding k-Best Perfect Matchings. *Discrete Applied Mathematics* 18, 2 (1987), 155–165.

[12] Wei-Ting Chiu, Pei Wang, and Patrick Shafto. 2022. Discrete Probabilistic Inverse Optimal Transport. In *ICML*. 3925–3946.

[13] Nicolas Courty, Rémi Flamary, Devis Tuia, and Alain Rakotomamonjy. 2016. Optimal Transport for Domain Adaptation. *TPAMI* 39, 9 (2016), 1853–1865.

[14] Marco Cuturi. 2013. Sinkhorn Distances: Lightspeed Computation of Optimal Transport. *NeurIPS* 26 (2013), 2292–2300.

[15] Yihe Dong and Will Sawin. 2020. COPT: Coordinated Optimal Transport on Graphs. *NeurIPS* 33 (2020), 19327–19338.

[16] Stefan Fankhauser, Kaspar Riesen, and Horst Bunke. 2011. Speeding up Graph Edit Distance Computation Through Fast Bipartite Matching. In *International Workshop on Graph-Based Representations in Pattern Recognition*. 102–111.

[17] Andreas Fischer, Ching Y. Suen, Volkmar Frinken, Kaspar Riesen, and Horst Bunke. 2013. A Fast Matching Algorithm for Graph-Based Handwriting Recognition. In *International Workshop on Graph-Based Representations in Pattern Recognition (Lecture Notes in Computer Science, Vol. 7877)*. 194–203.

[18] Karam Gouda and Mona Arafa. 2015. An Improved Global Lower Bound for Graph Edit Similarity Search. *Pattern Recognition Letters* 58 (2015), 8–14.

[19] Karam Gouda and Mosab Hassaan. 2016. CSI_GED: An Efficient Approach for Graph Edit Similarity Computation. In *2016 IEEE 32nd International Conference on Data Engineering (ICDE)*. IEEE, 265–276.

[20] Derek Justice and Alfred Hero. 2006. A Binary Linear Programming Formulation of The Graph Edit Distance. *TPAMI* 28, 8 (2006), 1200–1214.

[21] Jongik Kim. 2021. Boosting Graph Similarity Search through Pre-computation. In *Proceedings of the 2021 International Conference on Management of Data*. 951–963.

[22] Jongik Kim, Dong-Hoon Choi, and Chen Li. 2019. Inves: Incremental Partitioning-Based Verification for Graph Similarity Search.. In *EDBT*. 229–240.

[23] Soheil Kolouri, Se Rim Park, Matthew Thorpe, Dejan Slepcev, and Gustavo K Rohde. 2017. Optimal Mass Transport: Signal Processing and Machine-Learning Applications. *IEEE Signal Processing Magazine* 34, 4 (2017), 43–59.

[24] Ling Li, Siqiang Luo, Yuhai Zhao, Caihua Shan, Zhengkui Wang, and Lu Qin. 2023. COCLEP: Contrastive Learning-based Semi-Supervised Community Search. In *ICDE*. 2483–2495.

[25] Yongjiang Liang and Peixiang Zhao. 2017. Similarity Search in Graph Databases: A Multi-Layered Indexing Approach. In *ICDE*. 783–794.

[26] Yongjiang Liang and Peixiang Zhao. 2017. Similarity Search in Graph Databases: A Multi-layered Indexing Approach. In *2017 IEEE 33rd International Conference on Data Engineering (ICDE)*. IEEE, 783–794.

[27] Junfeng Liu, Min Zhou, Shuai Ma, and Lujia Pan. 2023. MATA*: Combining Learnable Node Matching with A* Algorithm for Approximate Graph Edit Distance Computation. In *CIKM*. 1503–1512.

[28] Facundo Mémoli. 2011. Gromov-Wasserstein Distances and The Metric Approach to Object Matching. *Foundations of Computational Mathematics* 11, 4 (2011), 417–487.

[29] Michel Neuhaus, Kaspar Riesen, and Horst Bunke. 2006. Fast Suboptimal Algorithms for The Computation of Graph Edit Distance. In *Joint IAPR International Workshops on Statistical Techniques in Pattern Recognition (SPR) and Structural and Syntactic Pattern Recognition (SSPR)*. 163–172.

[30] Hermina Petric Maretic, Mireille El Gheche, Giovanni Chierchia, and Pascal Frossard. 2019. GOT: An Optimal Transport Framework for Graph Comparison. *NeurIPS* 32 (2019), 13899–13910.
[31] Gabriel Peyré, Marco Cuturi, et al. 2019. Computational Optimal Transport: With Applications to Data Science. *Foundations and Trends® in Machine Learning* 11, 5-6 (2019), 355–607.
[32] Gabriel Peyré, Marco Cuturi, and Justin Solomon. 2016. Gromov-Wasserstein Averaging of Kernel and Distance Matrices. In *ICML*. 2664–2672.
[33] Chengzhi Piao, Tingyang Xu, Xiangguo Sun, Yu Rong, Kangfei Zhao, and Hong Cheng. 2023. Computing Graph Edit Distance via Neural Graph Matching. *PVLDB* 16, 8 (2023), 1817–1829.
[34] Shaima Qureshi et al. 2023. Limits of Depth: Over-Smoothing and Over-Squashing in GNNs. *Big Data Mining and Analytics* 7, 1 (2023), 205–216.
[35] Rishabh Ranjan, Siddharth Grover, Sourav Medya, Venkatesan Chakaravarthy, Yogish Sabharwal, and Sayan Ranu. 2022. Greed: A Neural Framework for Learning Graph Distance Functions. In *NeurIPS*. 22518–22530.
[36] Kaspar Riesen and Horst Bunke. 2008. IAM Graph Database Repository for Graph Based Pattern Recognition and Machine Learning. In *Joint IAPR International Workshops on Statistical Techniques in Pattern Recognition (SPR) and Structural and Syntactic Pattern Recognition (SSPR) (Lecture Notes in Computer Science, Vol. 5342)*. 287–297.
[37] Kaspar Riesen and Horst Bunke. 2009. Approximate Graph Edit Distance Computation by Means of Bipartite Graph Matching. *Image and Vision Computing* 27, 7 (2009), 950–959.
[38] Kaspar Riesen, Sandro Emmenegger, and Horst Bunke. 2013. A Novel Software Toolkit for Graph Edit Distance Computation. In *International Workshop on GraphBased Representations in Pattern Recognition*. 142–151.
[39] T Konstantin Rusch, Michael M Bronstein, and Siddhartha Mishra. 2023. A Survey on Oversmoothing in Graph Neural Networks. *arXiv preprint arXiv:2303.10993* (2023).
[40] Nino Shervashidze, Pascal Schweitzer, Erik Jan Van Leeuwen, Kurt Mehlhorn, and Karsten M Borgwardt. 2011. Weisfeiler-Lehman Graph Kernels. *Journal of Machine Learning Research* 12, 9 (2011), 2539–2561.
[41] Liangliang Shi, Jack Fan, and Junchi Yan. 2024. OT-CLIP: Understanding and Generalizing CLIP via Optimal Transport. In *ICML*. 1–22.
[42] Liangliang Shi, Zhaoqi Shen, and Junchi Yan. 2024. Double-Bounded Optimal Transport for Advanced Clustering and Classification. In *AAAI*, Vol. 38. 14982–14990.
[43] Liangliang Shi, Gu Zhang, Haoyu Zhen, Jintao Fan, and Junchi Yan. 2023. Understanding and Generalizing Contrastive Learning from The Inverse Optimal Transport Perspective. In *ICML*. 31408–31421.
[44] Andrew M Stuart and Marie-Therese Wolfram. 2020. Inverse Optimal Transport. *SIAM J. Appl. Math.* 80, 1 (2020), 599–619.
[45] Titouan Vayer, Laetitia Chapel, Rémi Flamary, Romain Tavenard, and Nicolas Courty. 2020. Fused Gromov-Wasserstein Distance for Structured Objects. *Algorithms* 13, 9 (2020), 212.
[46] Titouan Vayer, Nicolas Courty, Romain Tavenard, Laetitia Chapel, and Rémi Flamary. 2019. Optimal Transport for Structured Data with Application on Graphs. In *ICML*, Vol. 97. PMLR, 6275–6284.
[47] Cédric Villani et al. [n. d.]. *Optimal Transport: Old and New*. Vol. 338. Springer.
[48] Cédric Vincent-Cuaz, Rémi Flamary, Marco Corneli, Titouan Vayer, and Nicolas Courty. 2021. Semi-Relaxed Gromov-Wasserstein Divergence and Applications on Graphs. In *ICLR*. 1–14.
[49] Hanchen Wang, Rong Hu, Ying Zhang, Lu Qin, Wei Wang, and Wenjie Zhang. 2022. Neural Subgraph Counting with Wasserstein Estimator. In *SIGMOD*. 160–175.
[50] Jianwei Wang, Kai Wang, Xuemin Lin, Wenjie Zhang, and Ying Zhang. 2024. Neural Attributed Community Search at Billion Scale. *PACMMOD* 1, 4 (2024), 1–25.
[51] Runzhong Wang, Tianqi Zhang, Tianshu Yu, Junchi Yan, and Xiaokang Yang. 2021. Combinatorial Learning of Graph Edit Distance via Dynamic Embedding. In *CVPR*. 5241–5250.
[52] Xiaoli Wang, Xiaofeng Ding, Anthony K. H. Tung, Shanshan Ying, and Hai Jin. 2012. An Efficient Graph Indexing Method. In *ICDE*. 210–221.
[53] Alan Geoffrey Wilson. 1969. The Use of Entropy Maximising Models, in the Theory of Trip Distribution, Mode Split and Route Split. *Journal of Transport Economics and Policy* (1969), 108–126.
[54] Bing Xiao, Xinbo Gao, Dacheng Tao, and Xuelong Li. 2008. HMM-Based Graph Edit Distance for Image Indexing. *International Journal of Imaging Systems and Technology* 18, 2-3 (2008), 209–218.
[55] Shunxin Xiao, Shiping Wang, Yuanfei Dai, and Wenzhong Guo. 2022. Graph Neural Networks in Node Classification: Survey and Evaluation. *Machine Vision and Applications* 33, 1 (2022), 4–22.
[56] Hongteng Xu, Dixin Luo, and Lawrence Carin. 2019. Scalable Gromov-Wasserstein Learning for Graph Partitioning and Matching. In *NeurIPS*. 3046–3056.
[57] Jingjing Xu, Hao Zhou, Chun Gan, Zaixiang Zheng, and Lei Li. 2021. Vocabulary Learning via Optimal Transport for Neural Machine Translation. In *ACL*. 1–13.

[58] Keyulu Xu, Weihua Hu, Jure Leskovec, and Stefanie Jegelka. 2018. How Powerful Are Graph Neural Networks? *arXiv preprint arXiv:1810.00826* (2018).
[59] Lei Yang and Lei Zou. 2021. Noah: Neural-Optimized A* Search Algorithm for Graph Edit Distance Computation. In *ICDE*. 576–587.
[60] Weijie Yu, Zhongxiang Sun, Jun Xu, Zhenhua Dong, Xu Chen, Hongteng Xu, and Ji-Rong Wen. 2022. Explainable Legal Case Matching via Inverse Optimal Transport-based Rationale Extraction. In *SIGIR*. 657–668.
[61] Zhiping Zeng, Anthony KH Tung, Jianyong Wang, Jianhua Feng, and Lizhu Zhou. 2009. Comparing Stars: On Approximating Graph Edit Distance. *PVLDB* 2, 1 (2009), 25–36.
[62] Muhan Zhang. 2022. Graph Neural Networks: Link Prediction. *Graph Neural Networks: Foundations, Frontiers, and Applications* (2022), 195–223.
[63] Muhan Zhang and Yixin Chen. 2018. Link Prediction Based on Graph Neural Networks. *NeurIPS* 31 (2018), 5171–5181.
[64] Wei Zhang, Zihao Wang, Jie Fan, Hao Wu, and Yong Zhang. 2024. Fast Gradient Computation for Gromov-Wasserstein Distance. *Journal of Machine Learning* 3, 3 (2024), 282–299.
[65] Kangfei Zhao, Jeffrey Xu Yu, Hao Zhang, Qiyan Li, and Yu Rong. 2021. A Learned Sketch for Subgraph Counting. In *SIGMOD*. 2142–2155.
[66] Xiang Zhao, Chuan Xiao, Xuemin Lin, Qing Liu, and Wenjie Zhang. 2013. A Partition-Based Approach to Structure Similarity Search. *PVLDB* 7, 3 (2013), 169–180.
[67] Xiang Zhao, Chuan Xiao, Xuemin Lin, and Wei Wang. 2012. Efficient Graph Similarity Joins with Edit Distance Constraints. In *ICDE*. IEEE, 834–845.
[68] Xiang Zhao, Chuan Xiao, Xuemin Lin, Wenjie Zhang, and Yang Wang. 2018. Efficient Structure Similarity Searches: A Partition-based Approach. *The VLDB Journal* 27, 1 (2018), 53–78.
[69] Weiguo Zheng, Lei Zou, Xiang Lian, Dong Wang, and Dongyan Zhao. 2013. Graph Similarity Search with Edit Distance Constraint in Large Graph Databases. In *CIKM*. 1595–1600.
[70] Jie Zhou, Ganqu Cui, Shengding Hu, Zhengyan Zhang, Cheng Yang, Zhiyuan Liu, Lifeng Wang, Changcheng Li, and Maosong Sun. 2020. Graph Neural Networks: A Review of Methods and Applications. *AI Open* 1 (2020), 57–81.

Received July 2024; revised September 2024; accepted November 2024